HHS Public Access

Author manuscript

Dalton Trans. Author manuscript; available in PMC 2020 October 07.

Published in final edited form as:

Dalton Trans. 2019 October 07; 48(39): 14547–14565. doi:10.1039/c9dt03039e.

A Brief Overview of Metal Complexes as Nuclear Imaging Agents

Douglas S. MacPherson[1,2,*], **Kimberly Fung**[1,3,*], **Brendon E. Cook**[1,3], **Lynn C. Francesconi**[1,3], **Brian M. Zeglis**[1,2,3,4,5]

[1]Department of Chemistry, Hunter College of the City University of New York, New York, NY, 10028

[2]Ph.D. Program in Biochemistry, the Graduate Center of the City University of New York, New York, NY, 10016

[3]Ph.D. Program in Chemistry, the Graduate Center of the City University of New York, New York, NY, 10016

[4]Department of Radiology, Memorial Sloan Kettering Cancer Center, New York, NY, 10065

[5]Department of Radiology, Weill Cornell Medical College, New York, NY, 10065

Abstract

Metallic radionuclides have been instrumental in the field of nuclear imaging for over half a century. While recent years have played witness to a dramatic rise in the use of radiometals as labels for chelator-bearing biomolecules, imaging agents based solely on coordination compounds of radiometals have long played a critical role in the discipline as well. In this work, we seek to provide a brief overview of metal complex-based radiopharmaceuticals for positron emission tomography (PET) and single photon emission computed tomography (SPECT). More specifically, we have focused on imaging agents in which the metal complex itself rather than a pendant biomolecule or targeting moiety is responsible for the *in vivo* behavior of the tracer. This family of compounds contains metal complexes based on an array of different nuclides as well as probes that have been used for the imaging of a variety of pathologies, including infection, inflammation, cancer, and heart disease. Indeed, two of the defining traits of transition metal complexes — modularity and redox chemistry — have both been creatively leveraged in the development of imaging agents. In light of our audience, particular attention is paid to structure and mechanism, though clinical data is addressed as well. Ultimately, it is our hope that this review will not only educate readers about some of the seminal work performed in this space over the last 30 years but also spur renewed interest in the creation of radiopharmaceuticals based on small metal complexes.

Graphical Abstract

Corresponding Author: Phone: 1-212-896-0443. Fax: 1-212-896-0484. bz102@hunter.cuny.edu.

*These authors contributed equally to the preparation of this work.

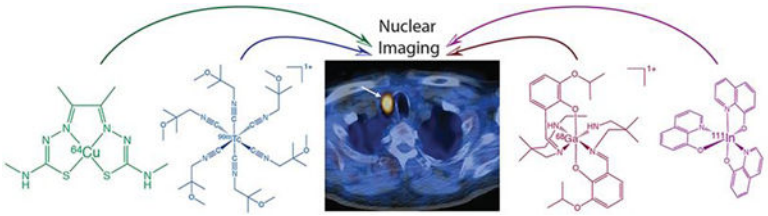

In this review, we seek to provide a brief and accessible overview of metal complex-based radiopharmaceuticals for nuclear imaging.

Keywords

Nuclear imaging; positron emission tomography; PET; single photon emission computed tomography; SPECT; inorganic chemistry; metal complex; radiometals; ^{99m}Tc; ^{111}In; ^{68}Ga; ^{67}Ga; ^{64}Cu; ^{86}Y; ^{89}Zr

INTRODUCTION

Over the past half-century, nuclear imaging has evolved from a largely experimental technique to a critical component of modern clinical practice. Single photon emission computed tomography (SPECT) and positron emission tomography (PET) have proven invaluable to oncology, cardiology, and neurology, providing functional imaging data that complements that produced by magnetic resonance imaging (MRI) and computed tomography (CT).

The centerpiece of any nuclear imaging technique is the radiopharmaceutical, the tracer designed to selectively and specifically localize in a tissue of interest. And the heart of any radiopharmaceutical is, *of course*, its gamma- or positron-emitting radionuclide. A wide array of radionuclides has been used in PET and SPECT tracers, including isotopes ranging from carbon-11 (^{11}C; $t_{1/2}$ ~ 20 min) to iodine-124 (^{124}I; $t_{1/2}$ ~ 4.2 d). The subset of *metallic* radionuclides — from here on called *radiometals* — has played an integral role in the field throughout its history (Table 1). Some of the earliest diagnostic imaging agents were complexes of technetium-99m (^{99m}Tc), while bioconjugates labeled with gallium-68 (^{68}Ga), copper-64 (^{64}Cu), and zirconium-89 (^{89}Zr) represent some of the most promising tracers today.[1] The vast majority of current research into radiometal-based imaging agents focuses on constructs in which a radiometal-chelate complex (*e.g.* [^{68}Ga]Ga-DOTA or [^{89}Zr]Zr-DFO) is appended to a delivery vector such as a small molecule, peptide, antibody, or nanoparticle.[2] Yet this, of course, is not the *only* flavor of radiometal-based imaging agent. Another class of probes exists in which the metal complex *itself* is the functional component of the imaging agent. In these, no additional targeting vector is needed, as the radiometal complex *alone* is responsible for the *in vivo* localization of the tracer. Three facets of coordination chemistry make radiometals a unique platform for the creation of nuclear imaging agents. First, the ability of metals to act as an anchor for a three-dimensional scaffold of ligands enables control over the structural, physical, and biological properties of the probe. Second, the modularity of metal-ligand interactions facilitates the screening and optimization of potential imaging agents. And third, the flexible redox chemistry of some

metal centers [*e.g.* Cu(I/II)] can provide an additional mechanism for the selective delivery of tracers to target tissues (though, to be fair, it has been a source of headaches as well).

Coordination complexes of a variety of radiometals have been used as nuclear imaging agents, and a handful of metal complex-based imaging agents have been translated to the clinic with varying degrees of success (Table 2). ^{99m}Tc is far and away the most commonly represented radiometal in this group, a fact that likely stems from the nuclide's popularity during the earliest days of nuclear medicine.[3] Enthusiasm for PET and SPECT tracers based on metal complexes has waned somewhat in recent years, a trend which has coincided with the rise of bioconjugates in the field. However, we strongly believe that metal complexes still have much to offer nuclear imaging. Furthermore, we contend that an accessible — though far from exhaustive — review of the topic could help spur interest and innovation in the field. Indeed, while a plethora of excellent reviews on the role of radiometals in nuclear imaging have been published in recent years — especially those of Blower[4], Donnelly[5], Orvig[6, 7], Bartholoma[8], Holland[9] and Boros[10]— the field has not seen an introductory, 'one-stop-shop' review specifically dedicated to the diversity of metal complex-based radiopharmaceuticals in quite a while.[1, 2, 4–6, 8, 9, 11–17]

In the pages that follow, we hope to offer an overview of the range of small metal complexes developed as PET and SPECT imaging agents, with a particular emphasis on work from the last twenty years. As we have discussed above, we have limited ourselves to agents in which the *in vivo* behavior of the tracer is predicated solely on the structure of the coordination complex *itself* rather than a pendant targeting functionality. This boundary condition excludes everything from radiometallated antibodies and nanoparticles to small metal complexes bearing hypoxia-targeting nitroimidazoles. While we have placed particular emphasis on structure and reactivity, clinical applications are discussed as well. Finally, in order to serve an audience of inorganic chemists, we have organized the work by radiometal rather than pathology, target, or mechanism. That said, further subdivisions were necessary within the section on ^{99m}Tc given the abundance of tracers based on the radiometal. Ultimately, it is our sincere hope that this work can play a part in fostering a revival of research into what we believe has become an underexplored class of nuclear imaging agents.

Technetium-99m

Introduction—The overwhelming majority of nuclear imaging agents based on small metal complexes are coordination compounds of ^{99m}Tc.[18] ^{99m}Tc is used in the vast majority of nuclear imaging scans and is presently the most widely used radionuclide in the clinic, largely due to its availability from the ^{99}Mo/^{99m}Tc generator. Furthermore, the physical characteristics of the radionuclide (E_γ = 140.5 keV; $t_{1/2}$ = 6.02 hours) are nearly ideal for SPECT imaging, and its short half-life and lack of particulate emissions result in minimal radiation burden to the patient. ^{99m}Tc decays to technetium-99 (^{99}Tc), a very weak β-emitter with an extraordinarily long half-life ($t_{1/2}$ ~ 211,000 y) that neither interferes with nor degrades image quality.[19]

The starting point for nearly all ^{99m}Tc-based radiopharmaceuticals is sodium pertechnetate: [^{99m}Tc]$NaTcO_4$.[20] Typically, pertechnetate is eluted from a generator and introduced directly into a "radiopharmaceutical kit". These kits generally contain a ligand, a reductant

— usually stannous ion — and a buffer, facilitating the creation of a solution that will yield the ^{99m}Tc-based imaging agent (it is important to note, however, that these kits often contain other components as well, including auxiliary ligands, catalysts, radical stabilizers, and compounds that aid in lyophilization). The advent of these radiopharmaceutical kits in the 1970s precipitated the rapid development of ^{99m}Tc-based SPECT agents for renal, myocardial, and hepatobiliary imaging. Unfortunately, however, the coordination chemistry of technetium was not well understood at the time, and, as a result, many early ^{99m}Tc-based radiopharmaceuticals were not fully characterized. Thankfully, studies of the coordination chemistry of technetium intensified in the late 1970s, leading to the discovery of an array of well-characterized ^{99m}Tc-based imaging agents with wide-ranging applications (Table 2).[21]

It is important to note that the concentration of [^{99m}Tc]TcO_4^- eluted from a generator is generally in the range of 10^{-7}–10^{-10} M. These remarkably low, “no-carrier-added” concentrations and the short half-life of ^{99m}Tc combine to preclude the characterization of ^{99m}Tc-complexes using routine analytical techniques available to inorganic chemists. In many cases, ^{99m}Tc’s long-lived isotopologue ^{99}Tc (β^-: 243 KeV) has enabled the use of standard macroscopic methods to determine the structure and physiochemical properties of ^{99m}Tc radiopharmaceuticals by proxy. Most of the ^{99m}Tc-based radiopharmaceuticals on the market since the 1980s have been characterized by synthesizing the ^{99}Tc isotopologue, studying the resulting complex using macroscopic analytical tools, and relating this data back to the ^{99m}Tc radiopharmaceutical via HPLC concordance experiments. Yet it is important to note that the discrete structures of some ^{99m}Tc-based radiopharmaceuticals remain unknown, particularly those based on ^{99m}Tc(III). In recent years, however, concerns over the storage and disposal of ^{99}Tc have curtailed the use of this approach. Today, rhenium, the third row congener of Tc, is increasingly used for structural characterization. However, two key differences between Re and Tc can cloud these results: the inertness of Re compared to Tc and the former’s higher reduction potential.

Over the years, imaging agents have been developed which feature the ^{99m}Tc cation in a wide variety of oxidation states. Consequently, in the pages that follow, we have divided our discussion according to the oxidation state of the metal center, beginning with Tc(I) and ending with Tc(V).

Tc(I) Complexes—Complexes of Tc(I) are inert, stable, and tend to prefer octahedral coordination geometries. Without question, the most well-known ^{99m}Tc(I)-based tracer is ^{99m}Tc(I)-hexakis(2-methoxy-2-methylpropyl)nitrile, informally known as [^{99m}Tc]Tc-MIBI or [^{99m}Tc]Tc-sestamibi (Figure 1). [^{99m}Tc]Tc-MIBI features a coordinatively inert Tc(I) center with a low-spin d^6 electron configuration surrounded by an octahedral array of six (2-methoxy-2-methylpropyl)nitrile ligands. The radiotracer is synthesized using a kit formulation in which the most important processes are metathesis and reduction reactions involving [^{99m}Tc]TcO_4^-, a preformed Cu(I)-tetrakis(2-methoxy-2-methylpropyl)nitrile complex, and a reducing agent (often $SnCl_2$).[22] The complex itself is positively charged (+1) and lipophilic and, as a result, accumulates in the mitochondria of cells.[22, 23] [^{99m}Tc]Tc-MIBI stands as the most successful variant of a large series of related compounds that were developed and optimized over a period of years.

Cardiac imaging is the principal clinical application of [^{99m}Tc]Tc-MIBI, and the uptake of the radiotracer in the myocardium is proportional to blood flow.[24] Consequently, clinicians can compare two [^{99m}Tc]Tc-MIBI scans taken under different conditions — one at rest, one during stress — in order to differentiate between induced and persistent abnormalities in myocardial perfusion. In the years since its emergence in nuclear cardiology, [^{99m}Tc]Tc-MIBI has found applications in other fields as well. For example, the uptake and retention of [^{99m}Tc]Tc-MIBI in breast cancer tissue has been explored as a predictive marker for response to chemotherapy.[25–27] Remarkably, [^{99m}Tc]Tc-MIBI — as well as a handful of other ^{99m}Tc(I) hexa-isonitrile compounds — has also been explored for both the imaging of parathyroid abnormalities as well as the delineation of the expression of p-glycoprotein (Pgp; multidrug resistance protein 1) (Figure 2).[28–31]

Of course, [^{99m}Tc]Tc-MIBI is not the only metal complex-based SPECT agent with a Tc(I) center. A handful of others have been developed, though none has advanced beyond preclinical investigations. For example, three different Tc(I)-tricarbonyl complexes have been reported as potential brain imaging agents: [^{99m}Tc]Tc-tricarbonyl 4-(*N*-benzylpiperdine)-pyridine-2-ylmthyl-amino acetic acid [^{99m}Tc][Tc(CO)$_3$PPAA], ^{99m}Tc tricarbonyl 4-iminodiacetato-*N*-benzylpiperdine [^{99m}Tc][Tc(CO)$_3$PipIDA]$^-$, and ^{99m}Tc tricarbonyl *N*-(2-mercapto-propyl)-1,2-phenylenediamine [^{99m}Tc][Tc(CO)$_3$MPPDA] (Figure 1).[32, 33] Unfortunately, however, initial preclinical investigations have revealed that each compound suffers from suboptimal uptake and retention in brain tissue. Perhaps more hopefully, another Tc(I)-tricarbonyl complex — [^{99m}Tc][Tc(CO)$_3$(NTA)]$^{2-}$ — was recently developed as an imaging agent to measure renal plasma flow (Figure 1).[34] The dianionic nature of the complex is thought to aid with plasma clearance, tubular extraction, and renal extraction. In preclinical studies, [^{99m}Tc][Tc(CO)$_3$(NTA)]$^{2-}$ has displayed higher uptake and retention in failed kidneys than the clinical gold standard: ^{131}I-*o*-iodohippurate. Finally, a family of ^{99m}Tc(I)-tricarbonyl complexes bearing tripodal tris(pyrazolyl)methane ligands — *e.g.* [^{99m}Tc][Tc(CO)$_3$(DMEOP)]$^+$ — has also been explored for imaging Pgp expression in preclinical models of breast and lung cancer (Figure 1).[35–37]

Tc(III) Complexes—A range of ^{99m}Tc(III) complexes has also been developed for SPECT imaging. ^{99m}Tc(III) complexes have a d^4 electron configuration and have been known to form 6- and 7-coordinate species with a wide variety of ligands. The best known of these tracers are the myocardial perfusion imaging agents [^{99m}Tc]Tc-teboroxime and [^{99m}Tc]Tc-Q12 (Figure 1).[38, 39] [^{99m}Tc]Tc-Teboroxime is the most successful agent to emerge from the boronic acid adducts of technetium dioximes (BATO) family of compounds.[38] The complex is heptacoordinate, featuring six imine donors and a (labile) chloride arranged around a ^{99m}Tc(III) center in a trigonal prismatic geometry.[40] Practically speaking, the neutral, lipophilic complex boasts rapid blood clearance and high uptake in myocardial tissue at early time points. In recent years, the Liu laboratory at Purdue University has sought to improve upon [^{99m}Tc]Tc-teboroxime through the creation of ‘second-generation’ variants with sulfonyl-containing boronate caps. One of these tracers — [^{99m}Tc]Tc-3SPboroxime — has displayed improved myocardial imaging properties compared to [^{99m}Tc]Tc-teboroxime, while another — [^{99m}Tc]Tc-4ASboroxime — has been shown to label red blood cells efficiently and displayed promise as a blood pool imaging agent in preclinical experiments.

[41, 42] [^{99m}Tc]Tc-Q12 — also known as [^{99m}Tc]Tc-furifosmin — is a member of the "Q-series" of six-coordinate compounds bearing two *trans* monodentate trialkylphosphine ligands as well as a tetradentate N_2O_2-based Schiff base ligand.[39] Like [^{99m}Tc]Tc-MIBI, [^{99m}Tc]Tc-Q12 is cationic and lipophilic and produces high uptake in myocardial tissue.[39, 43] Furthermore, like [^{99m}Tc]Tc-MIBI, [^{99m}Tc]Tc-Q12 — and the structurally related [^{99m}Tc]Tc-Q58 and [^{99m}Tc]Tc-Q63 complexes (Figure 1) — has also been used as a tracer for the delineation of Pgp expression.[44–46]

Moving on, [^{99m}Tc]Tc-DMSA is a hexacoordinate complex in which the ^{99m}Tc(III) center is bound by two tridentate dimercaptosuccinic acid ligands (Figure 1). The anionic, hydrophilic complex — which can be synthesized in a single step using a kit formulation — was developed as a renal imaging agent, as it accumulates in the cortical tubules and is eliminated via the urinary tract.[47] A ^{99m}Tc(V) version of [^{99m}Tc]Tc-DMSA is also accessible from the kit via an additional oxidation step (Figure 3).[48] Finally, a large family of iminodiacetic acid (IDA)-based complexes of ^{99m}Tc(III) — including the FDA-approved [^{99m}Tc]Tc-lidofenin, [^{99m}Tc]Tc-mebrofenin, and [^{99m}Tc]Tc-disofenin — have been developed for the SPECT imaging of the biliary tract (Figure 1).[49, 50] These tracers can be synthesized via a kit formulation and feature two tridentate diaryl iminodiacetic acid ligands arrayed around a ^{99m}Tc(III) center. The ability of this family of agents to image liver function arises from their uptake in hepatocytes and subsequent secretion into the bile.[51]

Tc(IV) Complexes—The members of the [^{99m}Tc]Tc-diphosphonate family of bone imaging agents are the best known tracers based on ^{99m}Tc(IV). [^{99m}Tc]Tc-MDP is the simplest member of this group, though its structure — most likely some sort of polymer in which methylenediphosphonate acts as a bridging ligand — remains elusive (Figure 3).[52] [^{99m}Tc]Tc-MDP, like all members of this family, relies upon the affinity of its phosphonate ligands for Ca^{2+} as the source of its affinity for bone.[53] A wide range of other ^{99m}Tc-labeled diphosphonates have been developed, including variants based on hydroxyethylidene diphosphonate (HEDP), hydroxymethylidene diphosphonate (HMDP), and pyrophosphate (Figure 3).[54] The quality of images obtained with these tracers can be ordered as follows: [^{99m}Tc]Tc-HMDP >> [^{99m}Tc]Tc-MDP > [^{99m}Tc]Tc-HEDP >> [^{99m}Tc]Tc-pyrophosphate (Figure 3). Recently, a new class of ^{99m}Tc-labeled diphosphonate tracers based on zoledronic acid has emerged, though the marginal improvement provided by these agents remains to be seen (Figure 3).[55, 56]

The reduction of [^{99m}Tc]TcO_4^- by reducing agents in the presence of weak ligands often forms ^{99m}Tc colloids that are presumed to be composed of ^{99m}Tc(IV). Thin layer chromatography methods have been developed to separate ^{99m}Tc-labeled complexes from both ^{99m}Tc-based colloids and [^{99m}Tc]TcO_4^-.[57] Though few ^{99m}Tc(IV) complexes have been identified for radiopharmaceutical purposes, a series of monocationic ^{99m}Tc(IV) complexes of *N*-substituted-3-hydroxy-2-methyl-4-pyridinones have been explored for renal imaging. Biodistribution studies in rabbits and mice show high uptake and retention in the kidneys, suggesting that these compounds may prove useful for kidney imaging.[58, 59] Finally, the ^{99m}Tc complex of the ubiquitous chelator diethylenetriaminepentaacetic acid ([^{99m}Tc]Tc-DTPA; Figure 3) has also been used clinically as a SPECT tracer for both kidney and brain imaging.[60, 61] Somewhat surprisingly, however, both the structure and the

oxidation state of [^{99m}Tc]Tc-DTPA have yet to be reliably determined, with the latter variously proposed to be ^{99m}Tc(III), ^{99m}Tc(IV), or ^{99m}Tc(V).[62]

Tc(V) Complexes—^{99m}Tc(V) complexes form the largest family of ^{99m}Tc-based SPECT tracers, and — not coincidentally — their history stretches back to the earliest days of ^{99m}Tc-SPECT. ^{99m}Tc(V) complexes have a d^2 electron configuration and, generally speaking, assume either 5-coordinate square pyramidal or 6-coordinate octahedral geometries in aqueous environments. Furthermore, most ^{99m}Tc(V) compounds can be divided into two categories: those containing [^{99m}Tc][Tc(V)=O]$^{3+}$ bonds and those containing [^{99m}Tc][Tc(V)≡N]$^{2+}$ bonds.

We will address complexes containing [^{99m}Tc][Tc(V)=O]$^{3+}$ bonds first, as these compounds have been more prevalent through the years. [^{99m}Tc]Tc(V)-propylene amine oxime ([^{99m}Tc]Tc-PnAO) was the first commercially available ^{99m}Tc-based cerebral blood flow agent approved for use in humans.[63] The neutral, distorted square pyramidal complex consists of a [^{99m}Tc][Tc(V)=O]$^{3+}$ motif and a diaminedioxime ligand (Figure 3).[63, 64] In order to compensate for the suboptimal pharmacokinetics of [^{99m}Tc]Tc-PnAO, a second-generation complex with a slightly altered ligand structure was created: [^{99m}Tc]Tc-hexamethylpropyleneamine oxime ([^{99m}Tc]Tc-HMPAO; Figure 3).[65, 66] [^{99m}Tc]Tc-HMPAO exists as two diastereomers: a *meso* compound and a pair of *d,l* enantiomers.[67] While the *meso* form diffuses quickly through the blood brain barrier, the *d,l* enantiomers decompose into hydrophilic products and are trapped in the brain, facilitating the imaging of cerebral perfusion.[67, 68] Interestingly, even after other agents have surpassed [^{99m}Tc]Tc-HMPAO's performance for brain imaging, its ability to label leukocytes has given the complex a second life as a whole-cell labeling reagent for intra-abdominal infections and inflammatory bowel disease.[69]

During the continued search for improved brain imaging agents, [^{99m}Tc]Tc-L,L-ethylenedicysteine diethylester ([^{99m}Tc]Tc-ECD) was identified as a lead candidate and subsequently approved for clinical use (Figure 3).[70] [^{99m}Tc]Tc-ECD is a neutral, lipophilic [^{99m}Tc][Tc(V)=O]$^{3+}$-containing diamide dimercaptide (N_2S_2) complex that was found to pass through the blood brain barrier and was subsequently approved for clinical use.[70] After the complex passes through the blood brain barrier, its two ester moieties are hydrolyzed by intracellular esterases, thereby creating a complex with a net negative charge.[71, 72] Due to differences in hydrolysis rates, the *l,l* isomer is retained in the brain, but the *d,d* isomer is not.[71, 72] Both isomers *are* hydrolyzed in the blood, however, ensuring rapid blood and renal clearance.[68, 73–75]

Continuing our discussion of N_xS_y complexes, in 1986, a series of ^{99m}Tc complexes with N_2S_2 ligands were explored as potential renal imaging agents.[76] Due to a variety of limitations, however, none of the complexes proved suitable. In response to this setback, the same team developed a ^{99m}Tc(V) complex bearing a triamide mercaptide (N_3S) ligand — mercaptoacetylglycylglycylglycine (MAG_3) — as an alternative (Figure 3).[76] [^{99m}Tc]Tc-MAG_3 is a negatively charged, square pyramidal complex boasting a [^{99m}Tc][Tc(V)=O]$^{3+}$ bond and a square pyramidal geometry.[76–78] Although 90% of [^{99m}Tc]Tc-MAG_3 is rapidly

bound to plasma protein after injection, 50% of the blood activity is excreted from the kidneys on each pass, making the radiotracer useful for measuring renal plasma flow.[79]

Despite the approval of [^{99m}Tc]Tc-MAG_3 by the U.S. FDA for renal perfusion imaging, its relatively high plasma protein binding meant that there was room for improvement.[80] During a study of [^{99m}Tc]Tc-ECD metabolites, it was found that the most polar of these metabolites — [^{99m}Tc]Tc-L,L-ethylenedicysteine ([^{99m}Tc]Tc-EC) — is rapidly excreted in the urine.[81] A subsequent study revealed that [^{99m}Tc]Tc-EC has a significantly lower blood plasma protein binding than [^{99m}Tc]Tc-MAG_3.[82] One drawback, however, was that it was found that at physiological pH, [^{99m}Tc]Tc-EC exists in both dianionic and monoanionic states, each of which exhibits a distinct clearance rate and protein binding affinity.[83] This complication was later overcome with the development of [^{99m}Tc]Tc-D-mercaptoacetamide-ethylene-cysteine ([^{99m}Tc]Tc-MAEC), which is an N_3S complex with a [^{99m}Tc][Tc(V)=O]$^{3+}$ motif that combines the most advantageous features of [^{99m}Tc]Tc-MAG_3 and [^{99m}Tc]Tc-EC (Figure 3).[84]

To wind down our discussion of agents containing [^{99m}Tc][Tc(V)=O]$^{3+}$ bonds, [^{99m}Tc][Tc(1,2-bis[bis(2-ethoxyethyl)phosphino]ethane)$_2O_2$]$^+$ — [^{99m}Tc]Tc-tetrofosmin — was developed in an effort to address concerns surrounding the non-target tissue uptake of ^{99m}Tc-based myocardial perfusion agents (Figure 3). [^{99m}Tc]Tc-tetrofosmin is a lipophilic, cationic, ^{99m}Tc(V) *trans*-dioxo bisdiphosphine complex bearing two terminal ethoxyethyl groups on each of its four phosphines.[85] The lipophilicity and dipole moment of the complex allows it to permeate the cytosolic membrane of heart cells.[86] After promising preclinical investigations, [^{99m}Tc]Tc-tetrofosmin was approved for use as a myocardial perfusion agent in the U.S. in 1996. Perhaps not surprisingly, [^{99m}Tc]Tc-tetrofosmin, like many myocardial perfusion imaging agents, has also been examined for the imaging of Pgp expression.[87, 88]

Shifting gears, in the mid-1990s, Pasqualini, *et al.* identified [^{99m}Tc]TcN[Et(EtO)NCS_2]$_2$ ([^{99m}Tc]Tc-NOET) as a potential myocardial perfusion imaging agent from a series of [^{99m}Tc][Tc(V)≡N]$^{2+}$-containing bisthiocarbamate complexes (Figure 3).[89] Although [^{99m}Tc]Tc-NOET was found to be reasonably effective for cardiac imaging, its clinical utility was ultimately limited by high non-target uptake in the lungs and liver as well as slow blood clearance.[90, 91] More recently, a wide range of [^{99m}Tc][Tc(V)≡N]$^{2+}$-based complexes has been explored as imaging agents. For example, the neutral, lipophilic complex containing a [^{99m}Tc][Tc(V)≡N]$^{2+}$ motif and two isopropyl xanthate (IPXT) ligands — [^{99m}Tc]TcN$(IPXT)_2$ — was found to have high brain uptake and retention (Figure 3).[92] In addition, the neutral lipophilic [^{99m}Tc][Tc(V)≡N]$^{2+}$-based complex formed from two 2,3-dimethylcyclohexl dithiocarbamato (DMCHDTC) ligands — [^{99m}Tc]TcN$(DMCHDTC)_2$ — and the cationic, lipophilic [^{99m}Tc][Tc(V)≡N]$^{2+}$-based complex containing one DMCHDTC ligand and one bis(dimethoxypropylphosphinoethyl)ethoxyethylamine (PNP5) ligand — [^{99m}Tc][TcN(PNP5)(DMCHDTC)]$^+$ — have both shown localization and retention in the heart, suggesting potential as myocardial imaging agents (Figure 3).[93, 94] In still another study, a [^{99m}Tc][Tc(V)≡N]$^{2+}$-based complex bearing two 4-dithiocarbamato-*N*-benylpiperidine (Pip-DTC) ligands was synthesized to create [^{99m}Tc][TcN]Pip-DTC, a tracer that displays affinity for sigma receptors *(Figure 3)*.[32]

Another member of the $[^{99m}Tc][Tc(V)\equiv N]^{2+}$ family — $[^{99m}Tc]$Tc-[bis(dimethoxypropylphosphinoethyl)-ethoxyethylamine-[bis(*N*-ethoxyethyl)-dithiocarbamato] nitride ($[^{99m}Tc]$TcN-DBODC$_5$) — has also been used as a myocardial perfusion imaging agent (Figures 3 and 4).[95–97] $[^{99m}Tc]$TcN-DBODC$_5$ is a monocationic ^{99m}Tc-nitrido complex containing a bidentate dithiocarbamate ligand and a tridentate PNP bisphosphine ligand arranged in an octahedral geometry. In preclinical experiments, $[^{99m}Tc]$TcN-DBODC$_5$ produced high uptake in the myocardium as well as lower liver-to-heart activity concentration ratios and faster blood clearance rates than both $[^{99m}Tc]$Tc-tetrosfosmin and $[^{99m}Tc]$Tc-MIBI.[98] Interestingly, $[^{99m}Tc]$TcN-DBODC$_5$'s selective mitochondrial accumulation and activity as a substrate for Pgp suggest that it may have a place in tumor imaging protocols as well.[99, 100] Like its compatriots, $[^{99m}Tc]$TcN-DBODC$_5$ is synthesized via kit formulation, though the need for post-kit purification has limited its clinical application. Another ^{99m}Tc(V)-based dithiocarbamate myocardial perfusion tracer — $[^{99m}Tc]$TcN-(DMCHDTC)$_2$ — was reported in 2009 by Zhang, *et al* (Figure 3).[94] Like $[^{99m}Tc]$TcN-DBODC$_5$, $[^{99m}Tc]$TcN-(DMCHDTC)$_2$ contains a $[^{99m}Tc][Tc(V)\equiv N]^{2+}$ motif, though the latter eschews phosphines for two tridentate dimethylcyclohexyl dithiocarbamate ligands. While preclinical investigations suggest that the *in vivo* performance of $[^{99m}Tc]$TcN-(DMCHDTC)$_2$ may compare favorably to other members of the $[^{99m}Tc]$Tc-dithiocarbamate family, no clinical studies have appeared to date. Finally, a related compound — $[^{99m}Tc][$TcN(*N*-ethoxyethyl-*N,N*-bis[2-(bis(3-methoxypropyl)phosphino)ethyl]amine)(2-mercaptopyridine oxide)$]^+$ ($[^{99m}Tc]$TcN-MPO) — has also recently been found to produce favorable myocardial uptake and improved liver-to-heart activity concentration ratios in both animals and humans (Figure 3).[101–103]

The Radioisotopes of Copper

Four radionuclides of copper have been used for PET imaging: ^{60}Cu ($t_{1/2}$ = 0.4 h; β^+ yield = 93%; $E_{\beta+}$ = 3.9 and 3.0 MeV), ^{61}Cu ($t_{1/2}$ = 3.32 h; β^+ yield = 62%; $E_{\beta+}$ = 1.2 and 1.15 MeV), ^{62}Cu ($t_{1/2}$ = 0.16 h; β^+ yield = 98%; $E_{\beta+}$ = 2.19 MeV), and ^{64}Cu ($t_{1/2}$ = 12.7 h; β^+ yield = 19%; $E_{\beta+}$ = 0.656 MeV).[104, 105] ^{64}Cu is easily the most often employed because it has a half-life that allows for facile handling and shipment and can be produced rather easily using a cyclotron via the bombardment of an enriched ^{64}Ni target. It is typically coordinated by chelators such as NOTA, SarAr, or CB-TE2A as part of a biomolecular conjugate. Regardless of the isotope, Cu(II) is the most biologically relevant oxidation state, though as we will see, reduction to Cu(I) is possible — and in some cases, desirable — *in vivo.* In light of its a d^9 electron configuration, Cu(II) can accommodate a variety of coordination numbers and geometries, including square planar, square pyramidal, trigonal bipyramidal, and octahedral.[104]

Thiosemicarbazones—The two most well-known Cu-based PET imaging agents are both small metal complexes of thiosemicarbazone ligands: Cu(II)-diacetyl-bis(N^4-thiosemicarbazone) [Cu-PTSM] and Cu(II)-diacetyl-bis(N^4-methylthiosemicarbazone) [Cu-ATSM] (Figure 5). In both cases, a Cu(II) center is coordinated in a square planar geometry by the two nitrogen atoms and two sulfur atoms of the thiosemicarbazone. Remarkably, while the structures of Cu-PTSM and Cu-ATSM only differ by a single methyl group, they have completely different applications: the former is a perfusion tracer, while the latter is

used for hypoxia imaging. Both complexes are prepared for the clinic using kit formulations and have been labeled and used with the entire gamut of radioisotopes of Cu.

Cu-PTSM is a radiotracer for the imaging of blood perfusion in the brain and myocardium.[105] Due to its small size, planarity, and lipophilicity, Cu-PTSM is able to move into cells via passive diffusion. While the exact mechanism of cellular uptake and retention remain subject to some debate, it is generally agreed upon that once inside the cell, the Cu(II) center is reduced to Cu(I) and subsequently dissociates from the PTSM ligand.[106, 107] Subsequently, this free Cu(I) binds to intracellular proteins, trapping Cu(I) within the cell. Preclinical studies in mice, non-human primates, and dogs all support the *in vivo* efficacy of Cu-PTSM for cerebral and myocardial perfusion imaging. In the clinic, Cu-PTSM has proven effective for the imaging of tumoral blood flow as well as both myocardial and cerebral perfusion. However, it has not been proven to provide any substantive advantages over other, more commonly-used perfusion imaging agents.[108–112]

As we have noted, Cu-PTSM's close cousin Cu-ATSM has an entirely different application: the imaging of hypoxia.[113] Briefly, the term 'hypoxic' is used to describe tissues that are deprived of normal, physiological levels of oxygen. In cancer, hypoxia is often associated with increased tumor aggressiveness, increased metastatic potential, higher rates of recurrence, and resistance to radiation therapy and chemotherapy. The selective uptake and retention of Cu-ATSM in hypoxic cells was first discovered in the late 1990s. Since then, a wealth of *in vitro* and *in vivo* data has supported the selectivity of the radiotracer, though variation has been observed between cell lines and tissue types.[114–120]

The precise mechanism of Cu-ATSM's uptake and retention in hypoxic cells has been subject to significant debate, though most agree that the reduction of the initial Cu(II) complex is a critical step.[120–122] Initially, it was believed that Cu(II)-ATSM could *only* be reduced and subsequently trapped in hypoxic tissues. However, Dearling *et al.* proposed a more nuanced mechanism. In this model, Cu(II)-ATSM is reduced in *both* hypoxic and normal tissues, producing a labile $[Cu(I)\text{-}ATSM]^-$ complex. In normoxic cells, this $[Cu(I)\text{-}ATSM]^-$ complex can be oxidized back to Cu(II)-ATSM, allowing the intact complex to diffuse out of the cell.[9] In hypoxic tissues, however, $[Cu(I)\text{-}ATSM]^-$ is not reoxidized rapidly enough to prevent its acid-catalyzed dissociation through [Cu(I)-ATSMH] or $[Cu(I)\text{-}ATSMH_2]^+$ intermediates, ultimately leading to the release and trapping of the radioactive Cu(I) by intracellular proteins.[123, 124] In 2005, Burgman *et al.* offered a hypothesis to explain why the uptake of Cu-ATSM varies between cell lines. The authors posited that because chaperones, transporters, and other proteins are required for the efflux and trapping of the radiotracer, variations in the expression levels of these proteins across cell lines will naturally lead to variations in hypoxia-selective uptake and retention.[125] Given the likely role of protonation in the acid-catalyzed dissociation reactions, intracellular pH differences between cell lines may also play a role in this variation. In light of this mechanistic work, it becomes clear that the disparity in hypoxia-selectivity between Cu-ATSM and Cu-PTSM is not solely predicated on the differing redox potentials of the two complexes (−0.59 and −0.51 V vs. Ag/AgCl, respectively) but also upon differences in their stabilities, protonation rates, and LUMO energies.[121] Mechanistic details aside, ^{60}Cu-, ^{62}Cu-, and ^{64}Cu-ATSM have all shown some promise in the clinic. In 2008, for example, Lewis *et al.* published a

trial comparing [^{60}Cu]Cu-ATSM and [^{64}Cu]Cu-ATSM PET in 10 patients with cervical carcinoma (Figure 6).[126] Increased uptake of both [^{60}Cu]Cu-ATSM and [^{64}Cu]Cu-ATSM was observed in the tumors of all 10 patients, though the authors reported that [^{64}Cu]Cu-ATSM produced higher quality images with superior tumor-to-background activity concentration ratios. However, neither [^{60}Cu]Cu-, [^{62}Cu]Cu-, nor [^{64}Cu]Cu-ATSM have been widely adopted for clinical hypoxia imaging to date.

In light of the limitations of Cu-ATSM and Cu-PTSM, a number of groups have worked on developing improved versions of these two tracers (Figure 5).[114, 116, 127–130] For example, Cu-ATSE, Cu-CTS, Cu-ASSM, Cu-ATSE/A-G, and Cu-ATSM/en were created as second-generation hypoxia imaging agents. Cu-ETS, Cu-$PTSM_2$, and Cu-PTS, on the other hand, were created as second-generation perfusion tracers. These novel tracers proved unable to appreciably improve upon the performance of their noteworthy precursors.

Interestingly, an additional family of ^{64}Cu-thiosemicarbazone complexes — Cu azabicyclo[3.2.2]nonane thiosemicarbazones — has been explored for yet another application: the *in vivo* delineation of topoisomerase II (Topo-II) expression (Figure 5).[131] Topoisomerase II is a DNA repair enzyme linked to increased tumor aggressiveness and metastatic potential in an array of cancers, and a number of Cu-thiosemicarbazone complexes have been shown to effectively inhibit Topo-II *in vitro. In vivo* experiments in mice bearing L1210 (Topo-II over-expressing) and PC-3 (Topo-II under-expressing) xenografts revealed that two of these ^{64}Cu-labeled complexes — [^{64}Cu]Cu-EPH144 and [^{64}Cu]Cu-EPH270 — produce specific tumoral uptake in the Topo-II over-expressing tumors. The translational potential of these two agents is limited by their very high accumulation in non-target tissues, but they nonetheless could serve as starting points for a second generation of optimized probes.[132]

Beyond Thiosemicarbazones—Moving away from thiosemicarbazone complexes, copper(I)-bis(diphosphine) complexes are well-characterized, lipophilic compounds with established tumoricidal properties (Figure 5). In 2000, Lewis *et al.* evaluated a series of ^{64}Cu-labeled Cu(I)-bis(diphosphine) complexes for the imaging of the multidrug resistance phenotype (MDR) in rats implanted with fibrocarcinoma.[133, 134] One of the complexes in question, [^{64}Cu][CuL^5_2]$^+$, was determined to accumulate in tumors with rapid clearance from the blood, renal excretion, and low uptake in non-target tissues. Unfortunately, however, no follow-up studies on this class of compounds have been published. Finally, a family of ^{64}Cu-based complexes bearing diiminedioxime ligands was also investigated as agents for both myocardial perfusion and MDR imaging, but few subsequent studies have emerged.[135, 136]

The Radioisotopes of Gallium

As with other radiometals, much of the recent work on ^{67}Ga- and ^{68}Ga-based imaging agents has made use of bifunctional chelators, placing it beyond the scope of this review. However, it is worth mentioning that one such agent — [^{68}Ga]Ga-DOTA-TATE — was recently approved by the FDA for the PET imaging of neuroendocrine tumors.[137, 138] Yet even though bioconjugate-based systems remain the primary focus of the field, the increased

availability and ease of use of ^{68}Ge/^{68}Ga-generators has sparked a surge of interest in ^{68}Ga-PET.[139] This trend, in turn, has led to the development of a handful of promising imaging agents based on small metal complexes.

Prior to the advent of [^{68}Ga]Ga-DOTA-TATE and its many cousins, the first prominent imaging agent based on gallium was [$^{67/68}$Ga]Ga-citrate.[140] [^{67}Ga]Ga-citrate was a common imaging agent for inflammation, infection, and certain types of tumors, including lung cancer, lymphoma, and leukemia, while [^{68}Ga]Ga-citrate has been used to visualize vascular permeability in lung disease as well as infections in the bone.[141] [$^{67/68}$Ga]Ga-citrate, however, is not stable *in vivo*; rather, the metal itself is quickly transchelated by transferrin to create [$^{67/68}$Ga]Ga-transferrin.[142] Consequently, the Ga-citrate complex *itself* is not essential to the *in vivo* localization of the radiopharmaceutical, thus excluding it from discussion here. Similarly, we will likewise eschew other unstable gallium complexes that rely upon transferrin for targeting.

Ligands with Oxygen, Nitrogen, and Sulfur Donors—Shifting gears to imaging agents that *do* fit our parameters, Li *et al.* first characterized gallium(III) N,N′-ethylene-di-L-cysteine (Ga-EC) in hopes of developing a new family of ^{67}Ga SPECT agents (Figure 7).[143] Ga-EC was found to have an $N_2S_2O_2$ distorted octahedral coordination in which nitrogen and sulfur atoms occupy the equatorial positions and oxygen atoms occupy the axial positions.[143] Although Ga-EC was shown to be stable under physiological conditions, [^{67}Ga]Ga-EC exhibited high liver uptake *in vivo* and was consequently abandoned as a prospective radiotracer. Years later, a mono-carboxylate derivative of EC — ethylenecysteamine cysteine (ECC) — was complexed with [^{68}Ga]Ga^{3+} to test its potential as a renal imaging agent homologous to [^{99m}Tc]Tc-ECC (Figure 7).[144] Although the structure of [^{67}Ga]Ga-ECC was not investigated, the authors proposed that the complex maintained the distorted octahedral geometry of Ga-EC, with an unknown ligand replacing the second carboxylate oxygen. Unlike [^{67}Ga]Ga-EC, [^{67}Ga]Ga-ECC primarily clears through the kidneys, a trait that led the investigators to test [^{68}Ga]Ga-ECC as a PET tracer for renal imaging.[145]

Ligands with Nitrogen and Sulfur Donors—More recently, the same laboratory that developed [^{67}Ga]Ga- and [^{68}Ga]Ga-ECC published a study focused on the use of a ^{68}Ga-labeled ethylcysteinate dimer ([^{68}Ga]Ga-ECD; Figure 7) as a cerebral blood flow PET tracer.[146] Generator-produced [^{68}Ga]$GaCl_3$ was reacted with a commercially available ECD kit to form the proposed — *though not confirmed* — cationic N_2S_2 complex. Although [^{68}Ga]Ga-ECD did not have sufficient uptake in the brain to allow for cerebral blood flow imaging, its relatively high cardiac uptake and fast urinary excretion indicate potential for myocardial perfusion imaging. $^{67/68}$Ga also forms stable complexes with the N_2S_2 ligand BAT-TECH, producing complexes that have exhibited high myocardial uptake in mice and non-human primates (Figure 7).[147, 148] X-ray crystallography of non-radioactive Ga-BAT-TECH revealed a 5-coordinate distorted square pyramidal geometry in which Ga^{3+} is bound to the tetradentate ligand as well as an axial chloride. While this structure was determined in the solid-state, it is likely that the chloride anion dissociates under physiological conditions, though this has not been investigated. Finally, Cutler, *et al.* explored the use of ^{68}Ga

complexes bearing tripodal NS_3 ligands for both brain and heart imaging (Figure 7)[149], while Moore and coworkers created an N_3S_3 framework — TX-TACNH$_3$ — that proved suitable for the stable coordination of both ^{111}In and $^{67/68}$Ga (Figure 7).[150, 151]

Ligands with Oxygen and Nitrogen Donors—Moving on to nitrogen- and oxygen-based ligands, gallium(III)-(bis(3-isopropoxy2-phenolate-benzylidene)-N,N'-bis(2,2-dimethyl-3-amino-propyl) ethylenediamine) — Ga[3-isopropoxy-ENBDMPI]$^+$ — is a hydrophobic, monocationic Ga(III)-complex with an N_4O_2 coordination sphere and a pseudo-octahedral geometry that has also been explored as a myocardial perfusion imaging agent (Figure 7).[152] Both [^{67}Ga]Ga- and [^{68}Ga]Ga-[3-isopropoxy-ENBDMPI]$^+$ have displayed high retention in the heart and rapid clearance from the liver, suggesting that these complexes could be deployed for cardiac SPECT and PET, respectively. In addition, Ga-[3-isopropoxy-ENBDMPI]$^+$ and several other structurally-related N_4O_2-based $^{67/68}$Ga complexes have also been investigated as functional imaging agents for multidrug resistance (MDR) and Pgp expression.[153–158]

Along similar lines, more than two decades ago, Green, *et al.* developed a series of $^{67/68}$Ga-labeled tracers using bis- and tris(salicylaldimine) platforms, most notably [$^{67/68}$Ga][Ga(4,6-MeO_2sal)$_2$BAPEN]$^+$ (Figure 7).[159–162] Several of these highly lipophilic, pseudo-octahedral N_3O_3-and N_4O_2-based complexes exhibited high myocardial uptake and rapid blood clearance in rats and dogs, though the *in vivo* results for a handful of these radiotracers in pigs revealed that the myocardial uptake was not proportional to perfusion, thereby precluding clinical translation.[162]

Interestingly, a series ^{68}Ga complexes with ligands based on curcumin ((1*E*,6*E*)-1,7-Bis(4-hydroxy-3-methoxyphenyl)hepta-1,6-diene-3,5-dione) has recently attracted attention for imaging β-amyloid plaques and fibrils in Alzheimer's disease. The three most promising of these ligands — curcumin (CUR), diacetyl-curcumin (DAC), and bis(dehydroxy)curcumin (bDHC) — were each found to form octahedral complexes with gallium(III) (Figure 7).[163–165] Although [^{68}Ga][Ga(CUR)$_2$(H_2O)$_2$]$^+$, [^{68}Ga][Ga(DAC)$_2$(H_2O)$_2$]$^+$, and [^{68}Ga][Ga(bDHC)$_2$(H_2O)$_2$]$^+$ all demonstrated a high affinity for β-amyloid plaques and fibrils *in vitro*, they unfortunately proved unable to produce useful images of amyloid aggregates *in vivo*. Yet in light of the potential benefits of PET imaging during early-stage Alzheimer's disease, it is likely that second-generation ^{68}Ga-curcuminoid complexes will be explored in search of a probe that combines high affinity for β-amyloid plaques and fibrils with favorable pharmacokinetic behavior.

In a very recent entry to this compendium, Greiser, *et al.* created a new class of ^{68}Ga-labeled radiotracers based on 1,4-diazepan-6-amine (DAZA) ligands.[166] These N_3O_3-based complexes are inert and stable, and while the preclinical data is sparing, *in ovo* imaging suggests that these compounds could serve as liver imaging agents. Finally, following the FDA approval of ^{153}Sm- and ^{177}Lu-ethylenediamine tetra(methylene phosphonic acid) (EDTMP) as bone-targeted radiotherapeutics, a ^{68}Ga-labeled variant of the compound ([^{68}Ga]Ga-EDTMP) has been tested as a PET imaging agent for bone scans (Figure 7).[167] [^{68}Ga]Ga-EDTMP has a putative octahedral geometry and an N_2O_4 coordination sphere and has shown rapid kidney clearance and high bone uptake in rat models.

Siderophores—Siderophore-derived ligands have also been used in conjunction with $^{67/68}$Ga to create bacteria-specific imaging agents.[168] Siderophores are molecules secreted into the extracellular space by some bacterial and fungal cells to scavenge essential ferric ions. Once these molecules find and bind the sought-after cations, they are actively transported back into the cell where the iron can be utilized for various cellular processes. In light of the metal ion-binding ability of many siderophores, inorganic radiochemists have jumped at the chance to harness these molecules for applications with radiometals. Some siderophores — most notably desferrioxamine — have emerged as the basis of bifunctional chelators. Others, however, have been leveraged to create infection-targeted imaging agents.

One laboratory in particular has made impressive preclinical advances in the radiolabeling of the fungal siderophore triacetylfusarinine C (TAFC) and the bacteria-derived siderophore ferrioxamine E (FOXE) for the imaging of invasive pulmonary aspergillosis (IPA).[168, 169] Both siderophores exhibit excellent binding to $^{68}Ga^{3+}$, which boasts coordination chemistry similar to their natural target Fe^{3+} (Figure 7). In fact, it was found that minimal degradation of [^{68}Ga]Ga-TAFC and [^{68}Ga]Ga-FOXE occurred even during competitive binding assays with Fe(III). *In vivo* PET imaging with these tracers in a rat model of IPA consistently showed uptake in the primary sites of infection (lungs) that was proportional to the severity of infection.[169] Just as importantly, both radiometal chelates showed visible accumulation in the lungs and clearance from the blood as soon as 20 minutes after their administration. However, assays testing the uptake of these ^{68}Ga-labeled siderophores by other species of bacteria and fungi found that not all had the same affinity for the imaging agents.[170] This suggests that different ^{68}Ga-siderophore complexes may be required to image different types of infections.

Indium-111 and Zirconium-89

Far and away the most common metal complex-based radiopharmaceuticals featuring ^{111}In ($t_{1/2}$ ~ 2.8 d) are reagents for cell labeling (Figure 8). The use of white blood cells for targeted imaging is predicated on the natural inclination of leukocytes and macrophages to migrate to sites of infection and inflammation within the body (Figure 9). Labeling these cells with ^{111}In-based metal complexes allows them to be tracked *in vivo* via SPECT. Clinically, this approach has been used to non-invasively visualize a range of pathologies, including fevers of unknown origin, post-operative infections, diabetic infections, and inflammation associated with cancer.[171–174] More recently, cell-labeling techniques have been harnessed as theranostic imaging strategies in conjunction with cell-based cancer therapies.[175] The incorporation of radionuclides into live, patient-derived neutrophils has been achieved by coordinating radiometals with lipophilic ligands, producing neutral, hydrophobic complexes that are passively taken up by cells. Upon diffusing through the cell membrane, the subsequent dissociation of the ligands frees the metal cation and allows it to bind to intracellular macromolecules, trapping it within the cytosol. These labeled autologous cells can then be administered to the patient, where they will resume their role as critical components of the immune system.

Two complexes have proven particularly effective for the labeling of a wide range of cell types: [^{111}In]In(oxinate)$_3$ and [^{111}In]In(tropolonate)$_3$ (Figure 8).[176–178] Though there has

been some debate regarding the relative merits of the two compounds, [^{111}In]In(oxinate)$_3$ — commonly known as ^{111}In-oxime — has been the more widely deployed in the clinic. The tropolonate complex labels cells somewhat more efficiently, which necessitates less preparation of the isolated neutrophils prior to labeling.[179] However, this difference has not proven significant enough to prompt a shift in clinical preference. It is important to note that while radioactive cell labeling has proven effective in the clinic, the use of ^{111}In has inherent limitations, most notably the nuclide's compatibility with SPECT rather than PET. To circumvent this issue, oxinate complexes of the positron-emitting radiometals ^{89}Zr and ^{68}Ga have recently been developed and studied in preclinical mouse models (Figure 8).[180–183]

CONCLUSION

In the preceding pages, we have sought to illuminate the remarkable breadth of metal complexes that have been used for PET and SPECT imaging. While we have tried to include many important and compelling examples, we are nonetheless sure that we have left out some excellent work. To the creators of these inadvertently neglected compounds, we humbly apologize and appeal to their understanding of the exigencies of writing introductory reviews.

As we mentioned in the introduction, the last two decades have been marked by a gradual decline in the development of radiopharmaceuticals based on metal complexes. Not surprisingly, this trend has run counter-parallel to the advent of biomolecular imaging agents labeled with radiometals. While we are firm believers in the power of peptides, proteins, and antibodies as targeting vectors, we nonetheless wonder if the pendulum has swung too far, leaving metal complex-based radiotracers with a regrettable lack of attention.

Meanwhile, the field of medicinal inorganic chemistry has recently undergone a fascinating surge.[184, 185] Researchers have increasingly harnessed the unique properties of transition metals to produce a wide range of complexes — including compounds centered on Ru, Au, Os, Ga, Co, and Fe — with potential as therapeutics for an array of diseases, most notably cancer.[186, 187, 188] For example, Meggers, *et al.* have developed a series of organometallic Ru(II) complexes that are potent kinase inhibitors (Figure 10, top).[189–191] In addition, the Jaouen laboratory has developed a family of organometallic Fe-based estrogen receptor modulators that has shown therapeutic potential in preclinical models of breast cancer (Figure 10, middle).[192–194] And finally, Patra, *et al.* have recently reported a novel class of organometallic iron- and chromium-based antibiotics based on the structure of platensimycin (Figure 10, bottom).[195–197] We contend that these compounds — and many others like them — represent fertile ground for the development of new diagnostic and theranostic radiopharmaceuticals. Some of these complexes are centered upon a metal (*e.g.* Cu) with at least one imaging-relevant isotopologue. Others, unfortunately, are not. In these cases, however, it would be possible to create a radiolabeled variant of the metal complex by incorporating a radionuclide such as ^{18}F or ^{11}C into a ligand either before or, preferably, after complexation. The radiolabeling of a ligand in the presence of a metal center may prove challenging, but we are confident that any difficulties could be circumvented, especially in light of the exciting recent advances in both ^{11}C and ^{18}F radiosynthesis.

In the end, it is our sincere hope that the coming years will play witness to a creative renaissance in the study of metal complexes for nuclear imaging and that work at the intersection of radiochemistry, molecular imaging, and medicinal inorganic chemistry will produce new generations of innovative and useful imaging agents.

ACKNOWLEDGEMENTS

The authors are grateful for the generous financial support of the National Institutes of Health (BMZ: R01CA204167, U01CA221046, and R01CA240963) and the National Science Foundation (DSM: HRD-1547830). We would also like to thank Professor John Babich (Weill Cornell Medical College) for helpful discussions and sage advice.

REFERENCES

1. Wadas TJ, Wong EH, Weisman GR and Anderson CJ, Chem. Rev, 2010, 110, 2858–2902. [PubMed: 20415480]
2. Zeglis BM and Lewis JS, Dalton Trans, 2011, 40, 6168–6195. [PubMed: 21442098]
3. Liu S and Chakraborty S, Dalton Trans, 2011, 40, 6077–6086. [PubMed: 21373664]
4. Blower PJ, Dalton Trans, 2015, 44, 4819–4844. [PubMed: 25406520]
5. Paterson BM and Donnelly PS, Chem. Soc. Rev, 2011, 40, 3005–3018. [PubMed: 21409228]
6. Price EW and Orvig C, Chem. Soc. Rev, 2014, 43, 260–290. [PubMed: 24173525]
7. Kostelnik TI and Orvig C, Chem. Rev, 2019, 119, 902–956. [PubMed: 30379537]
8. Bartholomä MD, Louie AS, Valliant JF and Zubieta J, Chem. Rev, 2010, 110, 2903–2920. [PubMed: 20415476]
9. Boros E and Holland JP, J Labelled Comp Radiopharm, 2018, 61, 652–671. [PubMed: 29230857]
10. Boros E and Packard AB, Chem. Rev, 2019, 119, 870–901. [PubMed: 30299088]
11. Morais GR, Paulo A and Santos I, Organometallics, 2012, 31, 5693–5714.
12. Kniess T, Laube M, Wüst F and Pietzsch J, Dalton Trans, 2017, 46, 14435–14451. [PubMed: 28829079]
13. Bhattacharyya S and Dixit M, Dalton Trans, 2011, 40, 6112–6128. [PubMed: 21541393]
14. Zeglis BM, Houghton JL, Evans MJ, Viola-Villegas N and Lewis JS, Inorg. Chem, 2014, 53, 1880–1899. [PubMed: 24313747]
15. Velikyan I, Med. Chem, 2011, 7, 345–379. [PubMed: 21711223]
16. Brandt M, Cardinale J, Aulsebrook ML, Gasser G and Mindt TL, J. Nucl. Med, 2018, 59, 1500–1506. [PubMed: 29748237]
17. Jurisson S, Cutler C and Smith SV, Q. J. Nucl. Med. Mol. Imaging, 2008, 52, 222–234. [PubMed: 18480740]
18. Mahmood A and Jones AG, Handbook of Radiopharmaceuticals, 2003, 323–362.
19. Holland JP, Williamson MJ and Lewis JS, Mol. Imaging, 2010, 9, 1–20. [PubMed: 20128994]
20. Welch MJand Redvanly CS, eds., Handbook of Radiopharmaceuticals: Radiochemistry and Applications, Wiley, New York, 2003.
21. Banerjee S, Pillai MR and Ramamoorthy N, Semin. Nucl. Med, 2001, 31, 260–277. [PubMed: 11710769]
22. Piwnica-Worms D, Kronauge JF and Chiu ML, Circulation, 1990, 82, 1826–1838. [PubMed: 2225379]
23. Chiu ML, Kronauge JF and Piwnica-Worms D, J. Nucl. Med, 1990, 31, 1646–1653. [PubMed: 2213187]
24. Jain D, Semin. Nucl. Med, 1999, 29, 221–236. [PubMed: 10433338]
25. Ciarmiello A, Del Vecchio S, Silvestro P, Potena MI, Carriero MV, Thomas R, Botti G, D'Aiuto G and Salvatore M, J. Clin. Oncol, 1998, 16, 1677–1683. [PubMed: 9586878]
26. Taillefer R, Semin. Nucl. Med, 1999, 29, 16–40. [PubMed: 9990681]

27. Waxman AD, Semin. Nucl. Med, 1997, 27, 40–54. [PubMed: 9122723]
28. Hendrikse NH, Franssen EJF, van der Graaf WTA, Meijer C, Piers DA, Vaalburg W and de Vries EGE, Br. J. Cancer, 1998, 77, 353–358. [PubMed: 9472628]
29. McBiles M, Lambert AT, Cote MG and Kim SY, Semin. Nucl. Med, 1995, 25, 221–234. [PubMed: 7570042]
30. Mendes F, Paulo A and Santos I, Dalton Trans, 2011, 40, 5377–5393. [PubMed: 21384018]
31. Keidar Z, Solomonov E, Karry R, Frenkel A, Israel O and Mekel M, Mol. Imag. Biol, 2017, 19, 265–270.
32. Satpati D, Bapat K, Dev Sarma H, Venkatesh M and Banerjee S, J. Labelled Compd. Radiopharmaceut, 2010, 53, 198–204.
33. Rattat D, Cleyhens B, Bormans G, Terwinghe C and Verbruggen A, Bioorg. Med. Chem. Lett, 2005, 15, 4192–4195. [PubMed: 16084082]
34. Lipowska M, Marzilli LG and Taylor AT, J. Nucl. Med, 2009, 50, 454–460. [PubMed: 19223406]
35. Fernandes C, Maria L, Gano L, Santos IC, Santos I and Paulo A, J. Organomet. Chem, 2014, 760, 138–148.
36. Maria L, Fernandes C, Garcia R, Gano L, Paulo A, Santos IC and Santos I, Dalton Trans, 2009, DOI: 10.1039/b817451b, 603–606.
37. Maria L, Cunha S, Videira M, Gano L, Paulo A, Santos IC and Santos I, Dalton Trans, 2007, DOI: 10.1039/b705226, 3010–3019. [PubMed: 17622418]
38. Zheng Y, Ji S, Tomaselli E, Ernest C, Freiji T and Liu S, Nucl. Med. Biol, 2014, 41, 813–824. [PubMed: 25169135]
39. Rossetti C, Vanoli G, Paganelli G, Kwiatkowski M, Zito F, Colombo F, Bonino C, Carpinelli A, Casati R, Deutsch K and et al., J. Nucl. Med, 1994, 35, 1571–1580. [PubMed: 7931652]
40. Treher EN, Francesconi LC, Gougoutas JZ, Malley MF and Nunn AD, Inorg. Chem, 1989, 28, 3411–3416.
41. Zhao Z-Q, Liu M, Fang W and Liu S, J. Med. Chem, 2018, 61, 319–328. [PubMed: 29186661]
42. Liu M, Zhao Z-Q, Fang W and Liu S, Bioconj. Chem, 2017, 28, 2998–3006.
43. Bernard BF, Krenning EP, Breeman WAP, Ensing G, Benjamins H, Bakker WH, Visser TJ and de Jong M, Nucl. Med. Biol, 1998, 25, 233–240. [PubMed: 9620628]
44. Ballinger JR, Muzzammil T and Moore MJ, J. Nucl. Med, 1997, 38, 1915–1919. [PubMed: 9430469]
45. Crankshaw CL, Marmion M, Luker GD, Rao V, Dahlheimer J, Burleigh BD, Webb E, Deutsch KF and Piwnica-Worms D, J. Nucl. Med, 1998, 39, 77–86. [PubMed: 9443741]
46. Luker GD, Crankshaw CL and Piwnica-Worms D, J. Nucl. Med, 1997, 38, 321–321.
47. Enlander D, Weber PM and dos Remedios LV, J. Nucl. Med, 1974, 15, 743–749. [PubMed: 4854105]
48. Ugur O, Kostakoglu L, Guler N, Caner B, Uysal U, Elahi N, Haliloglu M, Yuksel D, Aras T, Bayhan H and Bekdik C, Eur. J. Nucl. Med, 1996, 23, 1367–1371. [PubMed: 8781142]
49. Loberg MD, Cooper M, Harvey E, Callery P and Faith W, J. Nucl. Med, 1976, 17, 633–638. [PubMed: 1271111]
50. Chervu LR, Nunn AD and Loberg MD, Semin. Nucl. Med, 1982, 12, 5–17. [PubMed: 6281914]
51. Lamdie H, Cook AM, Scarsbrook A. f., Lodge JPA, Robinson PJ and Chowdhury FU, Clin. Radiol, 2011, 66, 1094–1105. [PubMed: 21861996]
52. Libson K, Deutsch E and Barnett BL, J. Am. Chem. Soc, 1980, 102, 2476–2478.
53. Pauwels EKJ and Stokkel MPM, Q. J. Nucl. Med, 2001, 45, 18–26. [PubMed: 11456371]
54. Wong KK and Piert M, J. Nucl. Med, 2013, 54, 590–599. [PubMed: 23482667]
55. Qiu L, Cheng W, Lin J, Luo S, Xue L and Pan J, Molecules, 2011, 16, 6165–6178. [PubMed: 21788926]
56. Qiu L, Lin J, Cheng W, Wang Y and Luo S, Med. Chem. Res, 2013, 22, 6154–6162.
57. Larson SK, Solomon HF, Caldwell WW and Abrams MJ, Bioconj. Chem, 1995, 6, 635–638.
58. Edwards DS, Liu S, Lyster DM, Poirier MJ, Vo C, Webb GA, Zhang Z and Orvig C, Nucl. Med. Biol, 1993, 20, 857–863. [PubMed: 8241998]

59. Edwards DS, Liu S, Poirier MJ, Zhang Z, Webb GA and Orvig C, Inorg. Chem, 1994, 33, 5607–5609.
60. Lorberboym M, Lampl Y and Sadeh M, J. Nucl. Med, 2003, 44, 1898–1904. [PubMed: 14660714]
61. Arnold RW, Subramanian G, McAfee JG, Blair RJ and Thomas FD, J. Nucl. Med, 1975, 16, 357–367. [PubMed: 1194986]
62. Nosco D and Beaty-Nosco J, Coord. Chem. Rev, 1999, 184, 91–123.
63. Volkert WA, Hoffman TJ, Seger RM, Troutner DE and Holmes RA, Eur. J. Nucl. Med, 1984, 9, 511–516. [PubMed: 6394334]
64. Fair CK, Troutner DE, Schlemper EO, Murmann RK and Hoppe ML, Acta Crystallographica Section C, 1984, 40, 1544–1546.
65. Leonard Holman B., Jones AG, Lister-James J, Davison A, Abrams MJ, Kirshenbaum JM, Tumeh SS and English RJ, J. Nucl. Med, 1984, 25, 1350–1355. [PubMed: 6334145]
66. Leonard J-P, Nowotnik DP and Neirinckx RD, J. Nucl. Med, 1986, 27, 1819–1823. [PubMed: 3491188]
67. Nowotnik DP, Canning LR, Cumming SA, Harrison RC, Higley B, Nechvatal G, Pickett RD, Piper IM, Bayne VJ, Forster AM, Weisner PS, Neirinckx RD, Volkert WA, Troutner DE and Holmes RA, Nucl. Med. Commun, 1985, 6, 499–506. [PubMed: 3877892]
68. Sharp PF, Smith FW, Gemmell HG, Lyall D, Evans NTS, Gvozdanovic D, Davidson J, Tyrrell DA, Pickett RD and Neirinckx RD, J. Nucl. Med, 1986, 27, 171–177. [PubMed: 3712035]
69. Roddie ME, Peters AM, Danpure HJ, Osman S, Henderson BL, Lavender JP, Carroll MJ, Neirinckx RD and Kelly JD, Radiology, 1988, 166, 767–772. [PubMed: 3340775]
70. Vallabhajosula S, Zimmerman RE, Picard M, Stritzke P, Mena I, Hellman RS, Tikofsky RS, Stabin MG, Morgan RA and Goldsmith SJ, J. Nucl. Med, 1989, 30, 599–604. [PubMed: 2497233]
71. Walovitch RC, Cheesman EH, Maheu LJ and Hall KM, J. Cereb. Blood Flow Metab, 1994, 14.
72. Walovitch RC, Hill TC, Garrity ST, Cheesman EH, Burgess BA, O'Leary DH, Watson AD, Ganey MV, Morgan RA and Williams SJ, J. Nucl. Med, 1989, 30, 1892–1901. [PubMed: 2809756]
73. Holman BL, Hellman RS, Goldsmith SJ, Mena IG, Leveille J, Gherardi PG, Moretti J-L, Bischof-Delaloye A, Hill TC, Rigo PM, Van heertum RL, Ell PJ, Buell U, De Roo MC and Morgan RA, J. Nucl. Med, 1989, 30, 1018–1024. [PubMed: 2661751]
74. Leveille J, Demonceau G, De Roo M, Rigo P, Taillefer R, Morgan RA, Kupranick D and Walovitch RC, J. Nucl. Med, 1989, 30, 1902–1910. [PubMed: 2809757]
75. Leveille J, Demonceau G and Walovitch RC, J. Nucl. Med, 1992, 33, 480–484. [PubMed: 1552328]
76. Eshima D, Taylor A, Fritzberg AR, Kasina S, Hansen L and Sorenson JF, J. Nucl. Med, 1987, 28, 1180–1186. [PubMed: 2955085]
77. Kasina S, Fritzberg AR, Johnson DL and Eshima D, J. Med. Chem, 1986, 29.
78. Rao TN, Adhikesavalu D, Camerman A and Fritzberg AR, J. Am. Chem. Soc, 1990, 112, 5798–5804.
79. Jafri RA, Britton KE, Nimmon CC, Solanki K, Al-Nahhas A, Bomanji J, Fettich J and Hawkins LA, J. Nucl. Med, 1988, 29, 147–158. [PubMed: 2964516]
80. Bubeck B, Brandau W, Weber E, Kalble T, Parekh N and Georgi P, J. Nucl. Med, 1990, 31, 1285–1293. [PubMed: 2143528]
81. Verbruggen AM, Nosco DL, Van Nerom CG, Bormans GM, Adriaens PJ and De Roo MJ, J. Nucl. Med, 1992, 33, 551–557. [PubMed: 1532419]
82. Van Nerom CG, Bormans GM, De Roo MJ and Verbruggen AM, Eur. J. Nucl. Med, 1993, 20, 738–746. [PubMed: 8223766]
83. Taylor A, Hansen L, Eshima D, Malveaux E, Folks R, Shattuck L, Lipowska M and Marzilli LG, J. Nucl. Med, 1997, 36, 821–826.
84. Taylor AT, Lipowska M, Hansen L, Malveaux E and Marzilli LG, J. Nucl. Med, 2004, 45, 885–891. [PubMed: 15136640]
85. Kelly JD, Forster AM, Higley B, Archer CM, Booker FS, Canning LR, Chiu KW, Edwards B, Gill HK, McPartlin M, Nagle KR, Latham IA, Pickett RD, Storey AE and Webbon PM, J. Nucl. Med, 1993, 34, 222–227. [PubMed: 8429340]

86. Platts EA, North TL, Pickett RD and Kelly JD, J. Nucl. Cardiol, 1995, 2, 317–326. [PubMed: 9420806]
87. Muzzammil T, Moore MJ and Ballinger JR, Cancer Biother. Radiopharm, 2000, 15, 339–346. [PubMed: 11041018]
88. Ballinger JR, J. Clin. Pharmacol, 2001,39S–47S. [PubMed: 11452727]
89. Pasqualini R, Duatti A, Bellande E, Comazzi V, Brucato V, Hoffschir D, Fagret D and Comet M, J. Nucl. Med, 1994, 35, 334–341. [PubMed: 8295007]
90. Uccelli L, Giganti M, Duatti A, Bolzati C, Pasqualini R, Cittanti C, Colamussi P and Piffanelli A, J. Nucl. Med, 1995, 36, 2075–2079. [PubMed: 7472602]
91. Johnson G III, Nguyen KN, Liu Z, Gao P, Pasqualini R and Okada RD, J. Nucl. Cardiol, 1997, 4, 217–225. [PubMed: 9199259]
92. Zhang J, Lin Y, Sheng X and Wang X, Appl. Radiat. Isot, 2009, 67.
93. Zhang J, Song Z, Jinfeng C and Wang X, Appl. Radiat. Isot, 2009, 67, 1661–1663. [PubMed: 19443233]
94. Zhang J, Song Z and Wang X, Appl. Radiat. Isot, 2009, 67, 577–580. [PubMed: 19128978]
95. Hatada K, Riou LM, Ruiz M, Yamamichi Y, Duatti A, Lima RL, Goode AR, Watson DD, Beller GA and Glover DK, J. Nucl. Med, 2004, 45, 2095–2101. [PubMed: 15585487]
96. Hatada K, Ruiz M, Riou LM, Lima RL, Goode AR, Watson DD, Beller GA and Glover DK, J. Nucl. Cardiol, 2006, 13, 779–790. [PubMed: 17174809]
97. Zhang W-C, Fang W, Li B, Wang X-B and He Z-X, Cardiology, 2009, 112, 89–97. [PubMed: 18583906]
98. Cittanti C, Uccelli L, Pasquali M, Boschi A, Flammia C, Bagatin E, Casali M, Stabin MG, Feggi L, Giganti M and Duatti A, J. Nucl. Med, 2008, 49, 1299–1304. [PubMed: 18632816]
99. Bolzati C, Carta D, Gandin V, Marzano C, Morellato N, Salvarese N, Cantore M and Colabufo NA, J. Biol. Inorg. Chem, 2013, 18, 523–538. [PubMed: 23543234]
100. Bolzati C, Cavazza-Ceccato M, Agostini S, Tokunaga S, Casara D and Bandoli G, J. Nucl. Med, 2008, 49, 1336–1344. [PubMed: 18632814]
101. Kim Y-S, Shi J, Zhai S, Hou G and Liu S, J. Nucl. Cardiol, 2009, 16, 571–579. [PubMed: 19288164]
102. Kim Y-S, Wang J, Broisat A, Glover DK and Liu S, J. Nucl. Cardiol, 2008, 15, 535–546. [PubMed: 18674722]
103. Gao S, Zhao G, Wen Q, Bai L, Chen B, Ji T, Ji B and Ma Q, Clin. Nucl. Med, 2014, 39, 14–19. [PubMed: 24300347]
104. Wadas TJ, Wong EH, Weisman GR and Anderson CJ, Curr. Pharm. Des, 2007, 13, 3–16. [PubMed: 17266585]
105. Blower PJ, Lewis JS and Zweit J, Nucl. Med. Biol, 1996, 23, 957–980. [PubMed: 9004284]
106. Fujibayashi Y, Taniuchi H, Wada K, Yonekura Y, Konishi J and Yokoyama A, Ann. Nucl. Med, 1995, 9, 1–5. [PubMed: 7779524]
107. Green MA, Mathias CJ, Welch MJ, McGuire AH, Perry D, Fernandez-Rubio F, Perlmutter JS, Raichle ME and Bergmann SR, J. Nucl. Med, 1990, 31, 1989–1996. [PubMed: 2266398]
108. Herrero P, Hartman JJ, Green MA, Anderson CJ, Welch MJ, Markham J and Bergmann SR, J. Nucl. Med, 1996, 37, 1294–1300. [PubMed: 8708759]
109. Herrero P, Markham J, Weinheimer CJ, Anderson CJ, Welch MJ, Green MA and Bergmann SR, Circulation, 1993, 87, 173–183. [PubMed: 8419005]
110. Holschneider D, Yang J, Sadler T, Galifianakis N, Bozorgzadeh M, Bading J, Conti P and Maarek J-M, Brain Res, 2008, 1234, 32–43. [PubMed: 18687316]
111. Flower MA, Zweit J, Hall AD, Burke D, Davies MM, Dworkin MJ, Young HE, Mundy J, Ott RJ, McCready VR, Carnochan P and Allen-Mersh TG, Eur. J. Nucl. Med, 2001, 28, 99–103. [PubMed: 11202458]
112. Liu J, Hajibeigi A, Ren G, Lin M, Siyambalapitiyage W, Liu ZS, Simpson E, Parkey RW, Sun XK and Oz OK, J. Nucl. Med, 2009, 50, 1332–1339. [PubMed: 19617332]
113. Vavere AL and Lewis JS, Dalton Trans, 2007, 4893–4902. [PubMed: 17992274]

114. Basken NE and Green MA, Nucl. Med. Biol, 2009, 36, 495–504. [PubMed: 19520290]
115. Basken NE, Mathias CJ and Green MA, J. Pharm. Sci, 2009, 98, 2170–2179. [PubMed: 18937368]
116. Blower PJ, Castle TC, Cowley AR, Dilworth JR, Donnelly PS, Labisbal E, Sowrey FE, Teat SJ and Went MJ, Dalton Trans, 2003, DOI: 10.1039/B307499D, 4416–4425.
117. Bourgeois M, Rajerison H, Guerard F, Mougin-Degraef M, Barbet J, Michel N, Cherel M and Faivre-Chauvet A, Nuc. Med. Rev. Cent. East. Eur, 2011, 14, 90–95.
118. Carlin S, Zhang H, Reese M, Ramos NN, Chen Q and Ricketts S-A, J. Nucl. Med, 2014, 55, 515–521. [PubMed: 24491409]
119. Fujibayashi Y, Cutler C, Anderson C, McCarthy D, Jones L, Sharp T, Yonekura Y and Welch M, Nucl. Med. Biol, 1999, 26, 117–121. [PubMed: 10096511]
120. Fujibayashi Y, Taniuchi H, Yonekura Y and Ohtani H, J. Nucl. Med, 1997, 38, 1155. [PubMed: 9225812]
121. Holland JP, Barnard PJ, Collison D, Dilworth JR, Edge R, Green JC and McInnes EJ, Chem. Eur. J, 2008, 14, 5890–5907. [PubMed: 18494010]
122. Vāvere AL and Lewis JS, Nucl. Med. Biol, 2008, 35, 273–279. [PubMed: 18355682]
123. Dearling JLJ, Lewis JS, Mullen GED, Rae MT, Zweit J and Blower PJ, Eur. J. Nucl. Med, 1998, 25, 788–792. [PubMed: 9662602]
124. Dearling JLJ, Lewis JS, Mullen GED, Welch MJ and Blower PJ, J. Biol. Inorg. Chem, 2002, 7, 249–259. [PubMed: 11935349]
125. Burgman P, O'Donoghue JA, Lewis JS, Welch MJ, Humm JL and Ling CC, Nucl. Med. Biol, 2005, 32, 623–630. [PubMed: 16026709]
126. Lewis JS, Laforest R, Dehdashti F, Grigsby PW, Welch MJ and Siegel BA, J. Nucl. Med, 2008, 49, 1177–1182. [PubMed: 18552145]
127. Bayly SR, King RC, Honess DJ, Barnard PJ, Betts HM, Holland JP, Hueting R, Bonnitcha PD, Dilworth JR, Aigbirhio FI and Christlieb M, J. Nucl. Med, 2008, 49, 1862–1868. [PubMed: 18927340]
128. Green MA, Mathias CJ, Willis LR, Handa RK, Lacy JL, Miller MA and Hutchins GD, Nucl. Med. Biol, 2007, 34, 247–255. [PubMed: 17383574]
129. Bonnitcha PD, Bayly SR, Theobald MBM, Betts HM, Lewis JS and Dilworth JR, J. Inorg. Biochem, 2010, 104, 126–135. [PubMed: 19932509]
130. Bonnitcha PD, Vāvere AL, Lewis JSand Dilworth JR, J. Med. Chem, 2008, 51, 2985–2991. [PubMed: 18416544]
131. Wei L, Easmon J, Nagi RK, Muegge BD, Meyer LA and Lewis JS, J. Nucl. Med, 2006, 47, 2034–2041. [PubMed: 17138747]
132. Zeglis BM, Divilov V and Lewis JS, J. Med. Chem, 2011, 54, 2391–2398. [PubMed: 21391686]
133. Lewis JS, Dearling JL, Sosabowski JK, Zweit J, Carnochan P, Kelland LR, Coley HM and Blower PJ, Eur. J. Nucl. Med, 2000, 27, 638–646. [PubMed: 10901449]
134. Lewis JS, Zweit J, Dearling JLJ, Rooney BC and Blower PJ, Chem. Commun, 1996, DOI: 10.1039/CC9960001093, 1093–1094.
135. Packard AB, Barbarics E, Kronauge JF, Treves ST and Jones A, Abstracts of Papers of the American Chemical Society, 1998, 215, U957–U958.
136. Packard AB, Kronauge JF, Day PJ and Treves ST, Nucl. Med. Biol, 1998, 25, 531–537. [PubMed: 9751419]
137. Otte A, Jermann E, Behe M, Goetze M, Bucher HC, Roser HW, Heppeler A, Mueller-Brand J and Maecke HR, Eur. J. Nucl. Med, 1997, 24, 792–795. [PubMed: 9211767]
138. Kayani I, Bomanji JB, Groves A, Conway G, Gacinovic S, Win T, Dickson J, Caplin M and Ell PJ, Cancer, 2008, 112, 2447–2455. [PubMed: 18383518]
139. Zhernosekov KP, Filosofov DV, Baum RP, Aschoff P, Bihl H, Razbash AA, Jahn M, Jennewein M and Rosch F, J. Nucl. Med, 2007, 48, 1741–1748. [PubMed: 17873136]
140. Banerjee SRand Pomper MG, Appl. Radiat. Isot, 2013, 76, 2–13. [PubMed: 23522791]

141. Nanni C, Errani C, Boriani L, Fantini L, Ambrosini V, Boschi S, Rubello D, Pettinato C, Mercuri M, Gasbarrini A and Fanti S, J. Nucl. Med, 2010, 51, 1932–1936. [PubMed: 21078801]
142. Gunasekera SW, King LJ and Lavender PJ, Clin. Chim. Acta, 1972, 39, 401–406. [PubMed: 4114559]
143. Li Y, Martell AE, Hancock RD, Reibenspies JH, Anderson CJ and Welch MJ, Inorg. Chem, 1996, 35, 404–414. [PubMed: 11666222]
144. Jalilian AR, Yousefnia H, Zolghadri S, Khoshdel MR, Bolourinovin F and Rahiminejad A, J. Radioanal. Nucl. Chem, 2010, 284, 49–54.
145. Mirzaei A, Jalilian AR, Aghanejad A, Mazidi M, Yousefnia H, Shabani G, Ardaneh K, Geramifar P and Beiki D, Nucl. Med. Mol. Imaging (2010), 2015, 49, 208–216.
146. Mirzaei A, Jalilian AR, Shabani G, Fakhari A, Akhlaghi M and Beiki D, J. Radioanal. Nucl. Chem, 2016, 307, 725–732.
147. Francesconi LC, Liu BL, Billings JJ, Carroll PJ, Graczyk G and Kung HF, J. Chem. Soc., Chem. Commun, 1991, 2, 94–95.
148. Kung HF, Liu BL, Mankoff D, Kung MP, Billings JJ, Francesconi L and Alavi A, J. Nucl. Med, 1990, 31, 1635–1640. [PubMed: 2213185]
149. Cutler CS, Giron MC, Reichert DE, Snyder AZ, Herrero P, Anderson CJ, Quarless DA, Koch SA and Welch MJ, Nucl. Med. Biol, 1999, 26, 305–316. [PubMed: 10363802]
150. Moore DA, Fanwick PE and Welch MJ, Inorg. Chem, 1990, 29, 672–676.
151. Moore DA, Fanwick PE and Welch MJ, Inorg. Chem, 1989, 28, 1504–1506.
152. Sharma V, Sivapackiam J, Harpstrite SE, Prior JL, Gu H, Rath NP and Piwnica-Worms D, PLoS One, 2014, 9.
153. Fellner M, Dillenburg W, Buchholz HG, Bausbacher N, Schreckenberger M, Renz F, Rosch F and Thews O, Mol. Imag. Biol, 2011, 13, 985–994.
154. Piwnica-Worms D and Sharma V, Curr. Top. Med. Chem, 2010, 10, 1834–1845. [PubMed: 20645914]
155. Sharma V, Beatty A, Wey SP, Dahlheimer J, Pica CM, Crankshaw CL, Bass L, Green MA, Welch MJ and Piwnica-Worms D, Chem. Biol, 2000, 7, 335–343. [PubMed: 10801474]
156. Sharma V, Prior JL, Belinsky MG, Kruh GD and Piwnica-Worms D, J. Nucl. Med, 2005, 46, 354–364. [PubMed: 15695797]
157. Thews O, Dillenburg W, Fellner M, Buchholz HG, Bausbacher N, Schreckenberger M and Rosch F, Eur. J. Nucl. Med. Mol. Imag, 2010, 37, 1935–1942.
158. Sharma V, Beatty A, Wey SP, Dahlheimer J, Pica CM, Crankshaw CL, Bass L, Green MA, Welch MJ and Piwnica-Worms D, Chem Biol, 2000, 7, 335–343. [PubMed: 10801474]
159. Tsang BW, Mathias CJ, Fanwick PE and Green MA, J. Med. Chem, 1994, 37, 4400–4406. [PubMed: 7996552]
160. Green MA, Welch MJ, Mathias CJ, Fox KAA, Knabb RM and Huffman JC, J. Nucl. Med, 1985, 26, 170–180. [PubMed: 3871475]
161. Tsang BW, Mathias CJ and Green MA, J. Nucl. Med, 1993, 34, 1127–1131. [PubMed: 8315489]
162. Tarkia M, Saraste A, Saanijoki T, Oikonen V, Vähäsilta T, Strandberg M, Stark C, Tolvanen T, Teräs M, Savunen T, Green MA, Knuuti J and Roivainen A, Nucl. Med. Biol, 2012, 39, 715–723. [PubMed: 22264857]
163. Asti M, Ferrari E, Croci S, Atti G, Rubagotti S, Iori M, Capponi PC, Zerbini A, Saladini M and Versari A, Inorg. Chem, 2014, 53, 4922–4933. [PubMed: 24766626]
164. Rubagotti S, Croci S, Ferrari E, Iori M, Capponi PC, Lorenzini L, Calza L, Versari A and Asti M, Int. J. Mol. Sci, 2016, 17.
165. Rubagotti S, Croci S, Ferrari E, Orteca G, Iori M, Capponi PC, Versari A and Asti M, J. Inorg. Biochem, 2017, 173, 113–119. [PubMed: 28511061]
166. Greiser J, Kühnel C, Görls H, Weigand W and Freesmeyer M, Dalton Trans, 2018, 47, 9000–9007. [PubMed: 29923561]
167. Mirzaei A, Jalilian AR, Badbarin A, Mazidi M, Mirshojaei F, Geramifar P and Beiki D, Ann. Nucl. Med, 2015, 29, 506–511. [PubMed: 25903357]

168. Petrik M, Haas H, Schrettl M, Helbok A, Blatzer M and Decristoforo C, Nucl. Med. Biol, 2012, 39, 361–369. [PubMed: 22172389]
169. Petrik M, Haas H, Dobrozemsky G, Lass-Florl C, Helbok A, Blatzer M, Dietrich H and Decristoforo C, J. Nucl. Med, 2010, 51, 639–645. [PubMed: 20351354]
170. Petrik M, Haas H, Laverman P, Schrettl M, Franssen GM, Blatzer M and Decristoforo C, Mol. Imag. Biol, 2014, 16, 102–108.
171. Schmidt KG, Rasmussen JW, Sorensen PG and Wedebye IM, Scand. J. Infect. Dis, 1987, 19, 339–345. [PubMed: 3616497]
172. Ascher NL, Ahrenholz DH, Simmons RL, Weiblen B, Gomez L, Forstrom LA, Frick MP, Henke C and McCullough J, Ann. Surg, 1979, 114, 386–392.
173. Johnson JE, Kennedy EJ, Shereff MJ, Patel NC and Collier BD, Foot Ankle Int, 1996, 17, 10–16. [PubMed: 8821280]
174. Love C and Palestro CJ, J. Nucl. Med. Technol, 2004, 32, 47–57. [PubMed: 15175400]
175. Stanton SE, Eary JF, Marzbani EA, Mankoff D, Salazar LG, Higgins D, Childs J, Reichow J, Dang YS and Disis ML, J. Immunother. Cancer, 2016, 4, 27–31. [PubMed: 27190628]
176. Segal AW, Arnot RN, Thakur ML and Lavender JP, Lancet, 1976, 2, 1056–1058. [PubMed: 62903]
177. Peters AM, Saverymuttu SH, Reavy HJ, Danpure HJ, Osman S and Lavender JP, J. Nucl. Med, 1983, 24, 39–44. [PubMed: 6848702]
178. Kotze HF, Heyns AD, Lotter MG, Pieters H, Roodt JP, Sweetlove MA and Badenhorst PN, J. Nucl. Med, 1991, 32, 62–66. [PubMed: 1899112]
179. Intenzo CM, Desai AG, Thakur ML and Park CH, J. Nucl. Med, 1987, 28, 438–441. [PubMed: 3106593]
180. Charoenphun P, Meszaros LK, Chuamsaamarkkee K, Sharif-Paghaleh E, Ballinger JR, Ferris TJ, Went MJ, Mullen GED and Blower PJ, Eur. J. Nucl. Med. Mol. Imag, 2015, 42, 278–287.
181. Ferris TJ, Charoenphun P, Meszaros LK, Mullen GED, Blower PJ and Went MJ, Dalton Trans, 2014, 43, 14851–14857. [PubMed: 25164373]
182. Enyedy EA, Doemoetoer O, Varga E, Kiss L, Trondl R, Hartinger CG and Keppler BK, J. Inorg. Biochem, 2012, 117, 189–197. [PubMed: 23089600]
183. Chitambar CR, Future Med. Chem, 2012, 4, 1257–1272. [PubMed: 22800370]
184. Louie AY and Meade TJ, Chem. Rev, 1999, 99, 2711–2734. [PubMed: 11749498]
185. Mjos KD and Orvig C, Chem. Rev, 2014, 114, 4540–4563. [PubMed: 24456146]
186. Gianferrara T, Bratsos I and Alessio E, Dalton Trans, 2009, 7588–7598. [PubMed: 19759927]
187. Gasser G, Ott I and Metzler-Nolte N, J. Med. Chem, 2011, 54, 3–25. [PubMed: 21077686]
188. Bruijnincx PCA and Sadler PJ, Curr. Opin. Chem. Biol, 2008, 12, 197–206. [PubMed: 18155674]
189. Debreczeni JE, Bullock AN, Atilla GE, Williams DS, Bregman H, Knapp S and Meggers E, Angew. Chem. Int. Ed, 2006, 45, 1580–1585.
190. Feng L, Geisselbrecht Y, Blanck S, Wilbuer A, Atilla-Gokcumen GE, Filippakopoulos P, Kraeling K, Celik MA, Harms K, Maksimoska J, Marmorstein R, Frenking G, Knapp S, Essen L-O and Meggers E, J. Am. Chem. Soc, 2011, 133, 5976–5986. [PubMed: 21446733]
191. Smalley KSM, Contractor R, Haass NK, Kulp AN, Atilla-Gokcumen GE, Williams DS, Bregman H, Flaherty KT, Soengas MS, Meggers E and Herlyn M, Cancer Res, 2007, 67, 209–217. [PubMed: 17210701]
192. Jaouen G, Top S, Vessieres A, Leclercq G and McGlinchey MJ, Curr. Med. Chem, 2004, 11, 2505–2517. [PubMed: 15379709]
193. Top S, Vessieres A, Cabestaing C, Laios I, Leclercq G, Provot C and Jaouen G, J. Organomet. Chem, 2001, 637, 500–506.
194. Vessieres A, Top S, Beck W, Hillard E and Jaouen G, Dalton Trans, 2006, DOI: 10.1039/b509948f, 529–541.
195. Patra M, Gasser G and Metzler-Nolte N, Dalton Trans, 2012, 41, 6350–6358. [PubMed: 22411216]

196. Patra M, Gasser G, Pinto A, Merz K, Ott I, Bandow JE and Metzler-Nolte N, ChemMedChem, 2009, 4, 1930–1938. [PubMed: 19784974]

197. Patra M, Gasser G, Wenzel M, Merz K, Bandow JE and Metzler-Nolte N, Organometallics, 2010, 29, 4312–4319.

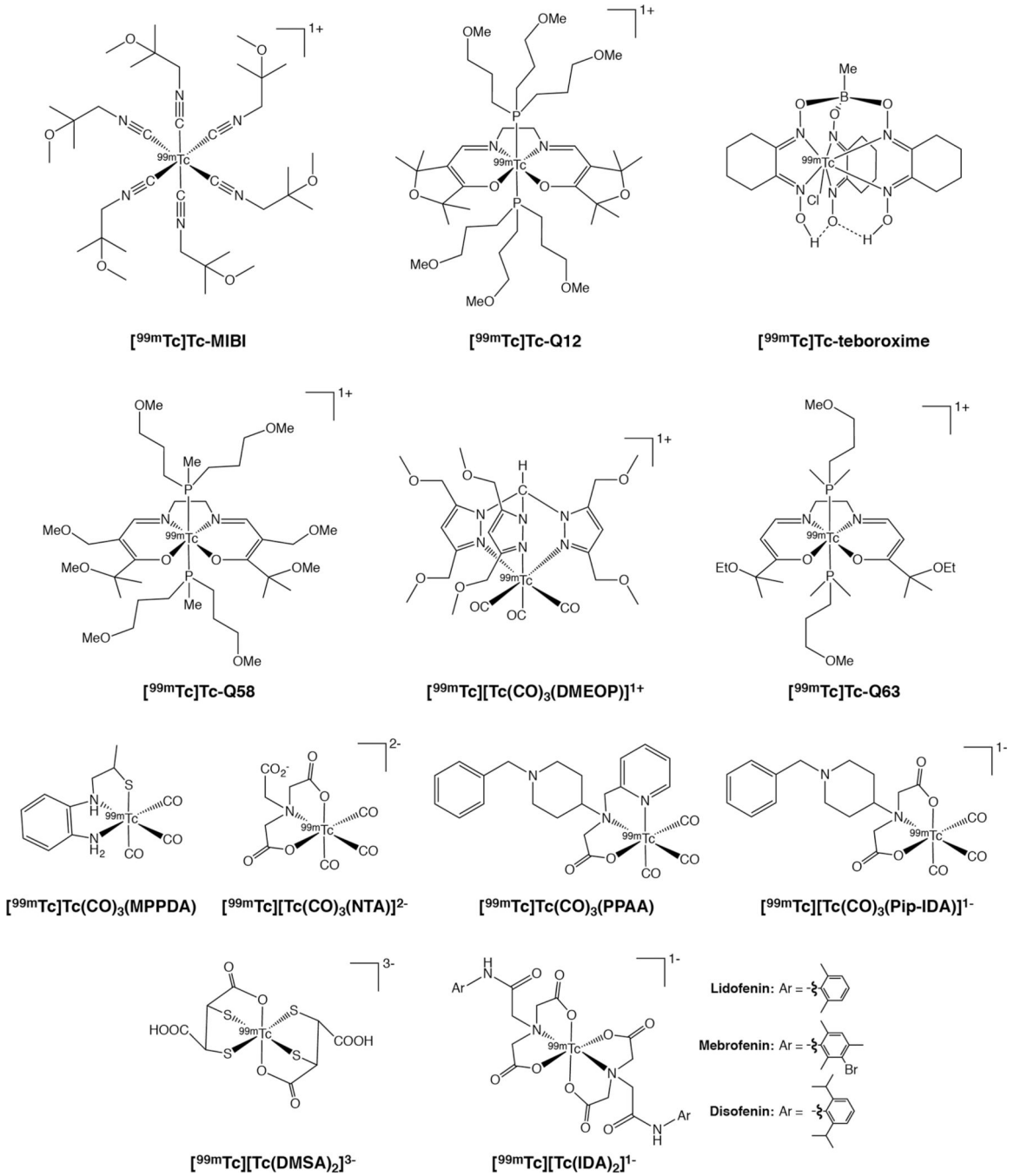

Figure 1.
Selected [^{99m}Tc]Tc(I) and [^{99m}Tc]Tc(III) complexes

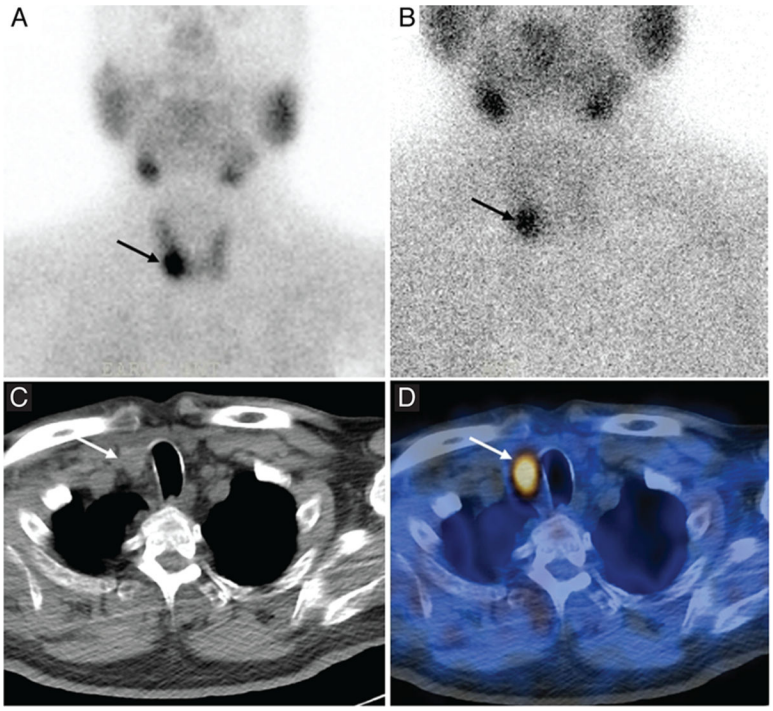

Figure 2.

Planar [^{99m}Tc]Tc-MIBI scintigraphy (A and B), CT (C), and SPECT/CT (D) of a patient with primary hyperparathyroidism, showing focal tracer uptake in the lower part of the right lobe of the thyroid gland. Reprinted from Keidar, *et al.* Preoperative [^{99m}Tc]Tc-MIBI SPECT/CT interpretation criteria for localization of parathyroid adenomas — correlation with surgical findings. *Molecular Imaging and Biology* **2017**, 19, 265–270. Copyright by the World Molecular Imaging Society.[31]

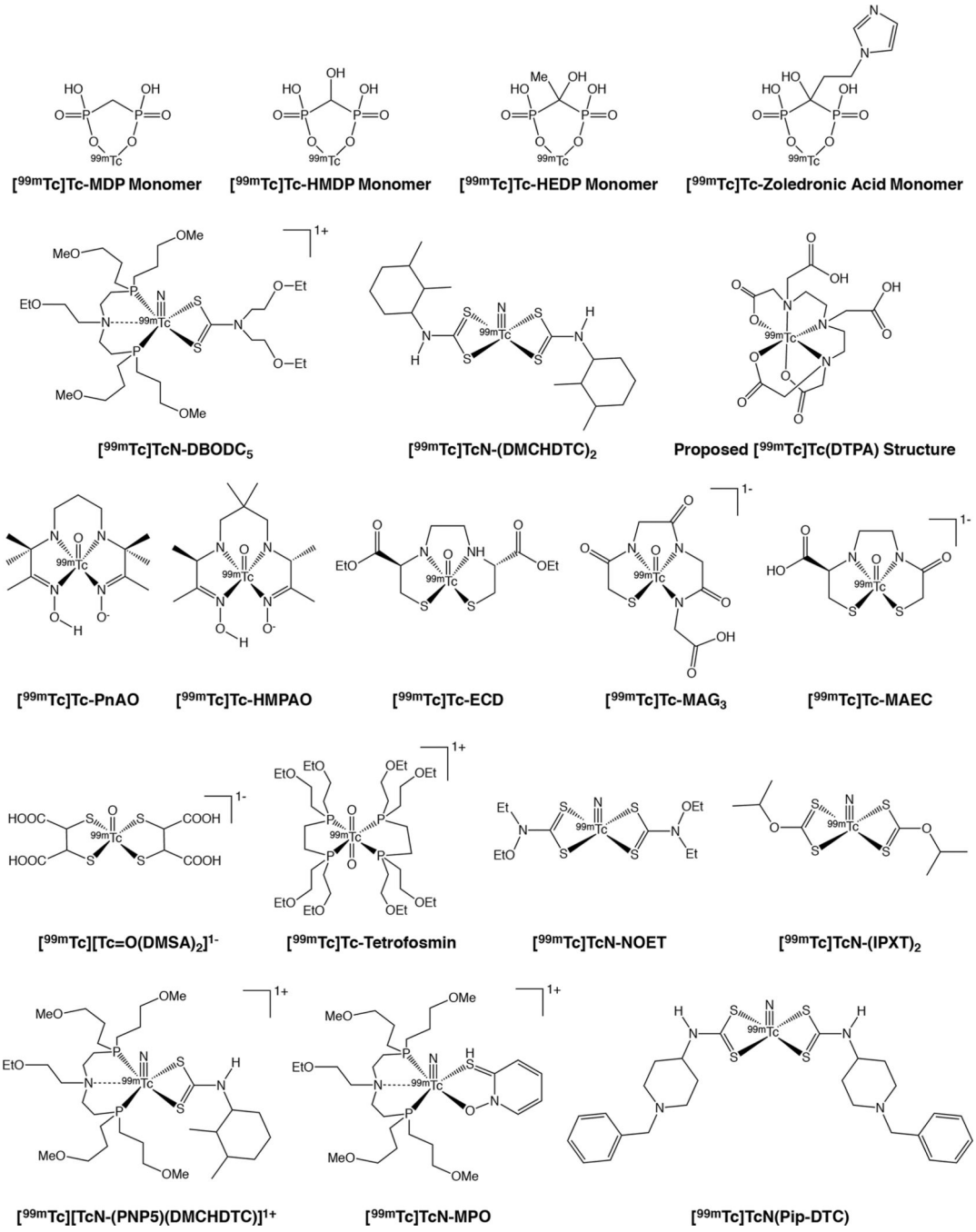

Figure 3.
Selected [^{99m}Tc]Tc(IV) and [^{99m}Tc]Tc(V) complexes

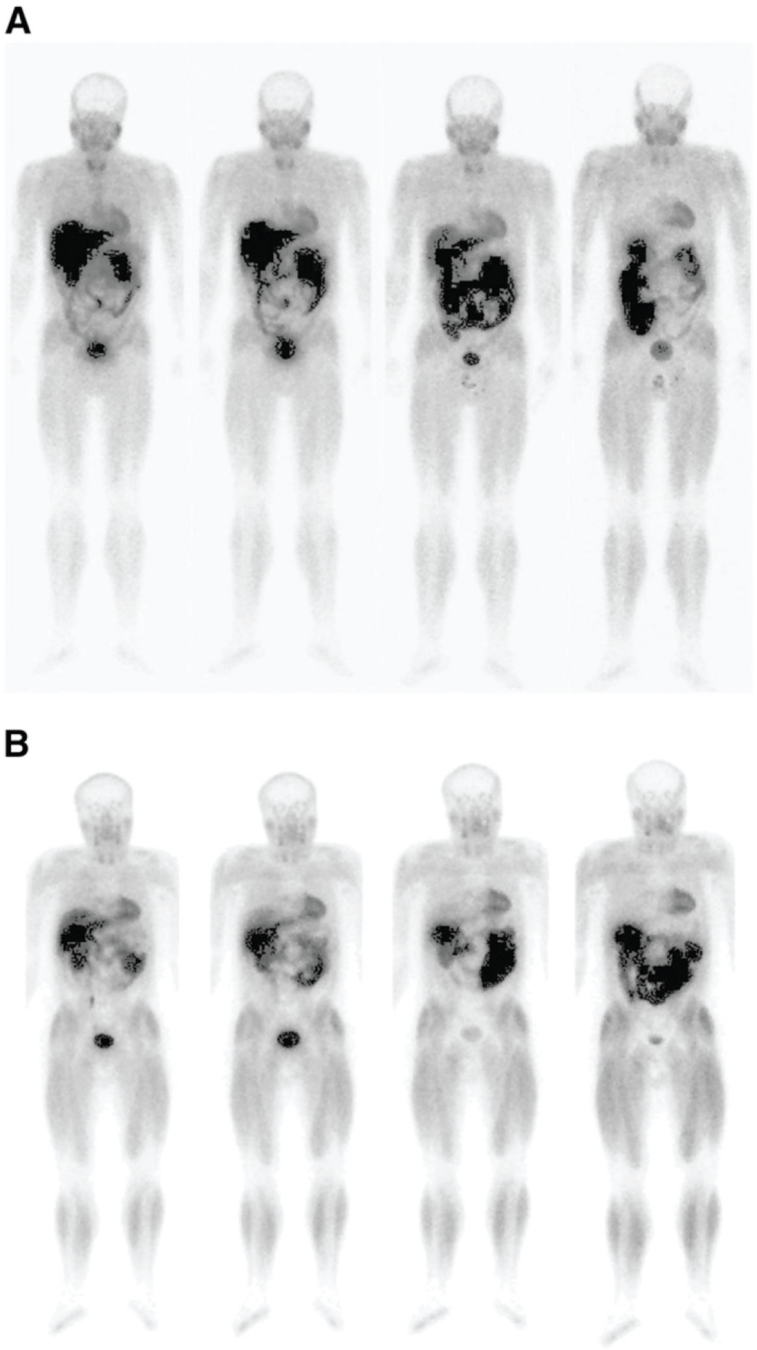

Figure 4.

Planar, whole-body [^{99m}Tc]TcN-DBODC$_5$ scintigraphy (left to right: collected 5, 30, 60, and 240 min post-injection) of a healthy under (A) rest and (B) stress conditions. Adapted and reprinted from Cittanti *et al.* Whole-body biodistribution and radiation dosimetry of the new cardiac tracer ^{99m}TcN-DBODC. *Journal of Nuclear Medicine* **2008**, *49*, 1299–1304. Copyright by the Society of Nuclear Medicine and Molecular Imaging.[98]

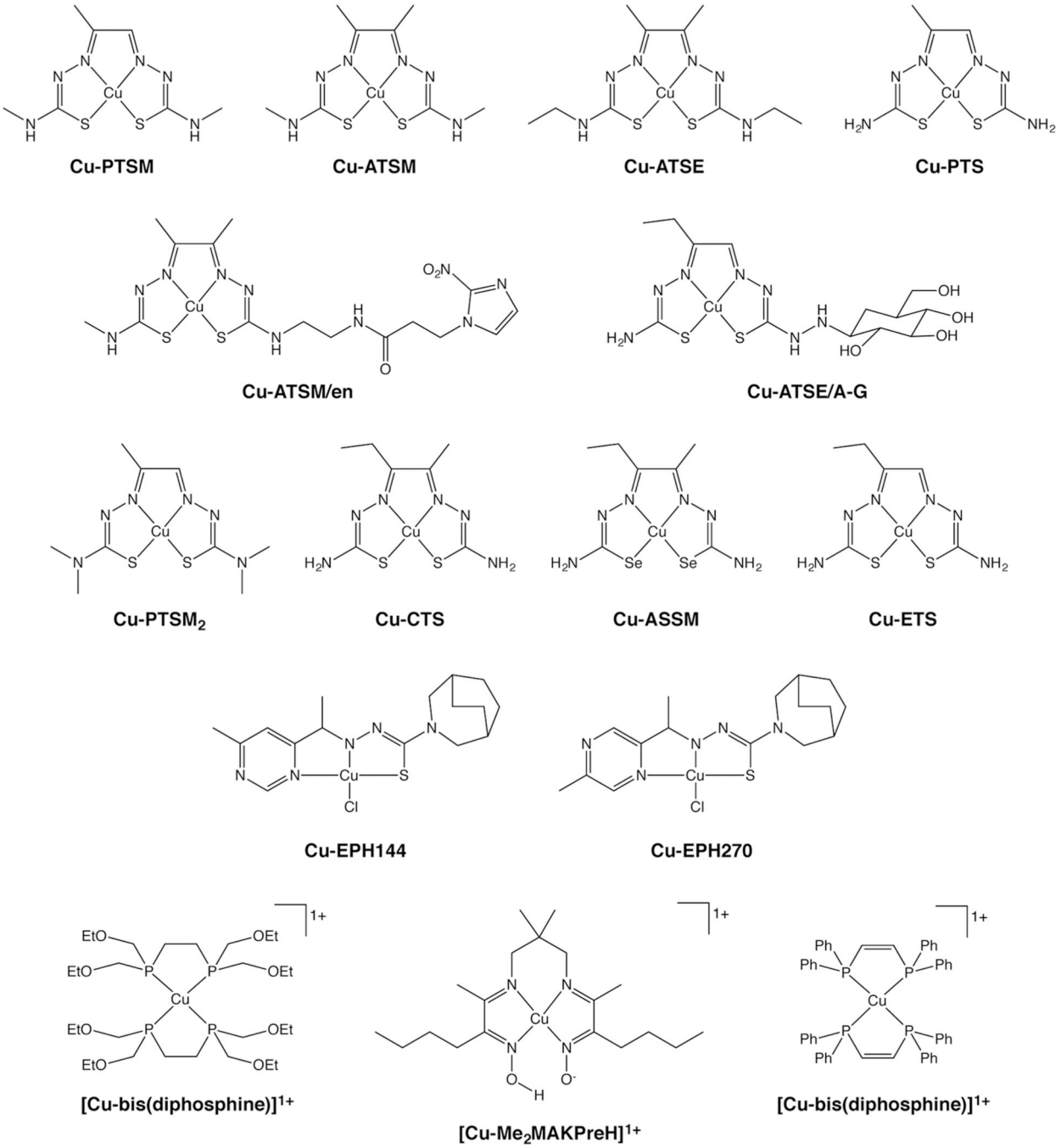

Figure 5.
Selected Cu(II) complexes

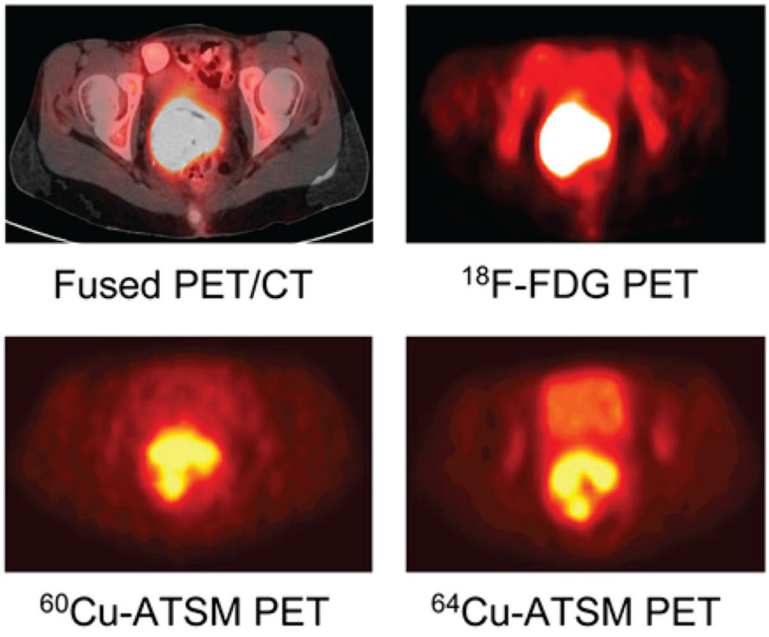

Figure 6.

Transaxial [^{18}F]FDG-PET/CT, [^{18}F]FDG PET, [^{60}Cu]Cu-ATSM PET, and [^{64}Cu]Cu-ATSM images of a patient with cancer of the uterine cervix. ^{18}F-FDG = [^{18}F]fluorodeoxyglucose = 2-deoxy-2-[^{18}F]fluoroglucose. Adapted and reprinted from Lewis *et al.* An imaging comparison of [^{64}Cu]Cu-ATSM and [^{60}Cu]Cu-ATSM in cancer of the uterine cervix. *Journal of Nuclear Medicine* **2008**, *49* (7), 1177–1182. Copyright by the Society of Nuclear Medicine and Molecular Imaging.[131]

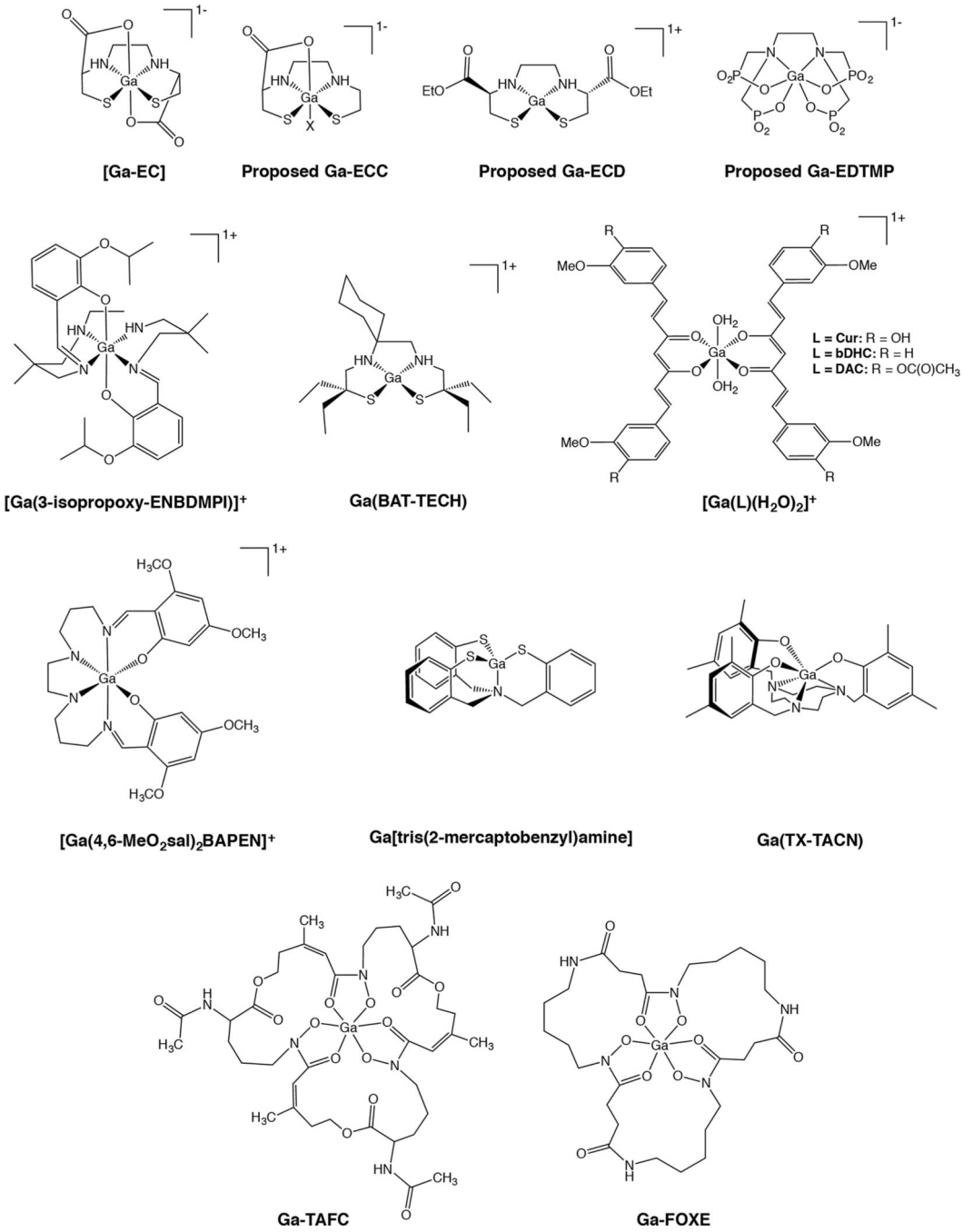

Figure 7.
Selected Ga(III) complexes

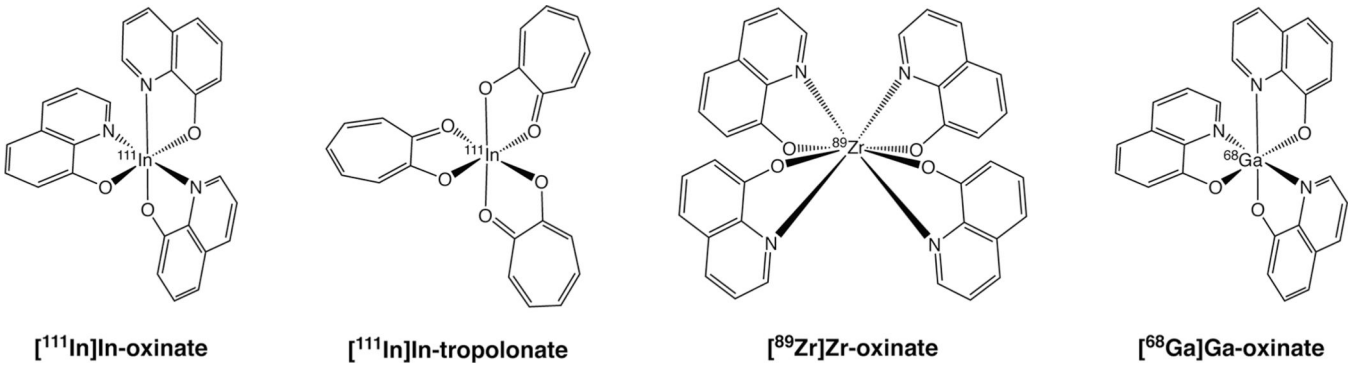

Figure 8.
Selected [^{111}In]In(III), [^{89}Zr]Zr(IV), and [^{68}Ga]Ga(III) complexes

Figure 9.

Planar scintigraphy using [^{111}In]In-oxine-labeled leukocytes revealing an area of increased uptake in an infected prosthetic vascular graft in the right thigh (black arrows). Adapted and reprinted from Love *et al.* Radionuclide imaging of infection. *Journal of Nuclear Medicine Technology* **2004**, *32*, 47–57. Copyright by the Society of Nuclear Medicine and Molecular Imaging.[174]

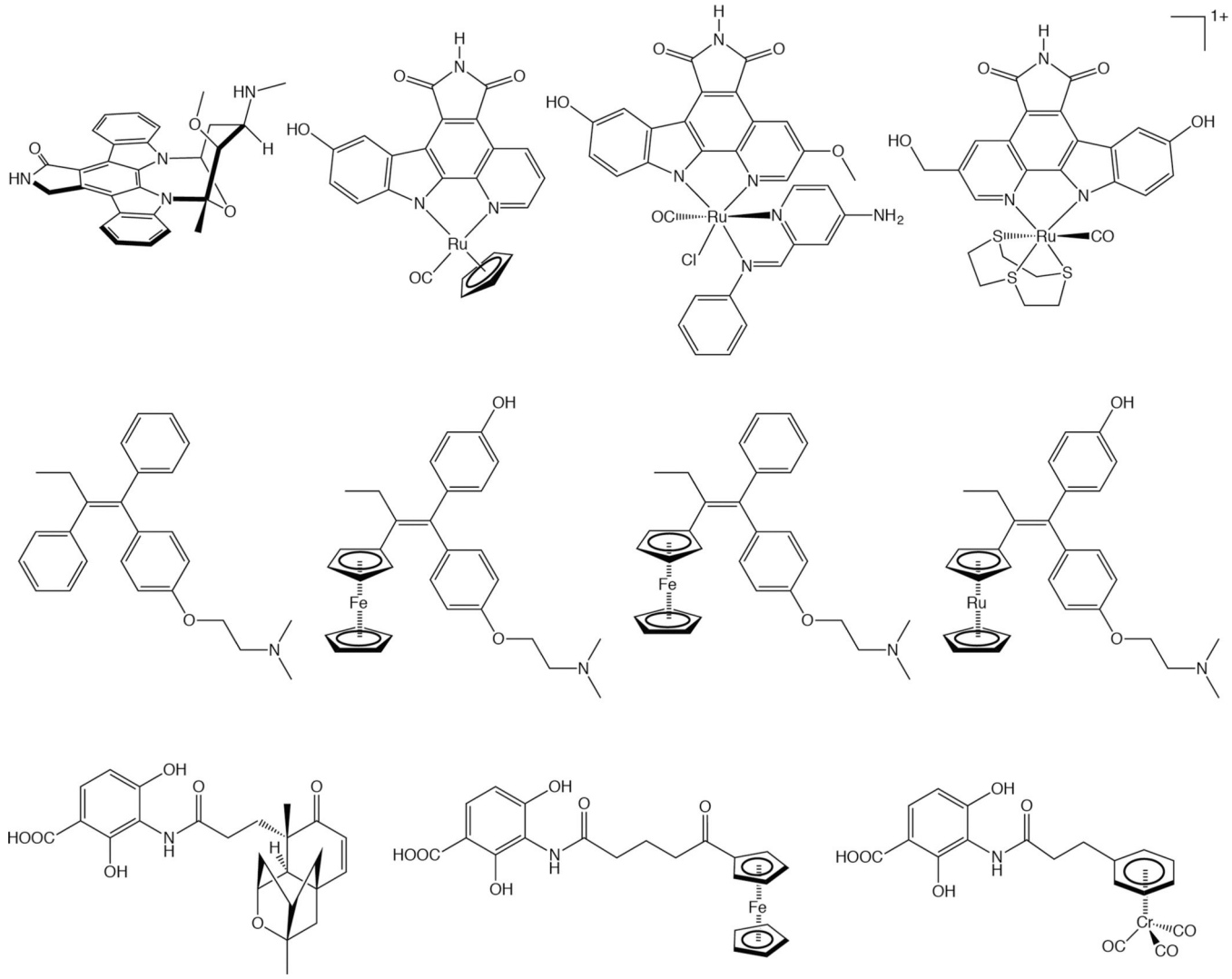

Figure 10.

Selected medicinal inorganic and organometallic compounds. Top: Ru-based kinase inhibitors inspired by the structure of staurosporine (far left). Middle: Fe- and Ru-based selective estrogen receptor modulators inspired by the structure of tamoxifen (far left). Bottom: Fe- and Cr-based antibiotics based on the structure of platensimycin (far left).

Table 1.

Chemical and physical properties of selected metallic radionuclides.

Modality	Nuclide	Half-Life	Source	Relevant Oxidation States	Common Coordination Number
PET	^{68}Ga	68 min	generator	3+	4, 5, 6
	^{60}Cu	23.7 min	cyclotron	1+, 2+	4, 5, 6
	^{61}Cu	3.3 h	cyclotron	1+, 2+	4, 5, 6
	^{62}Cu	9.7 min	cyclotron	1+, 2+	4, 5, 6
	^{64}Cu	12.7 h	cyclotron	1+, 2+	4, 5, 6
	^{86}Y	14.7 h	cyclotron	3+	8, 9
	^{89}Zr	78.4 h	cyclotron	4+	8
SPECT	^{99m}Tc	6.0 h	generator	1- to 7+	4, 5, 6
	^{111}In	67.3 h	cyclotron	3+	4, 5, 6
	^{67}Ga	78.2 h	cyclotron	3+	5, 6, 7, 8

Table 2.

Selected metal complex-based radiopharmaceuticals that have been translated to the clinic

Radiopharmaceutical	Clinical Application
$[^{99m}Tc][Tc(CO)_3(NTA)]^{2-}$	Renal perfusion
$[^{99m}Tc]TcN\text{-}DBODC_5$	Myocardial perfusion
$[^{99m}Tc]$Tc-disofenin	Hepatobiliary imaging
$[^{99m}Tc]$Tc-DMSA	Renal clearance; glioblastoma
$[^{99m}Tc]$Tc-DTPA	Bone metastasis
$[^{99m}Tc]$Tc-ECD	Brain perfusion
$[^{99m}Tc]$Tc-ECDG	Lung cancer
$[^{99m}Tc]$Tc-HEDP	Bone metastasis
$[^{99m}Tc]$Tc-HMDP	Bone metastasis
$[^{99m}Tc]$Tc-HMPAO	Brain perfusion
$[^{99m}Tc]$Tc-lidofenin	Hepatobiliary imaging
$[^{99m}Tc]$Tc-MAEC	Renal imaging
$[^{99m}Tc]Tc\text{-}MAG_3$	Renal perfusion
$[^{99m}Tc]$Tc-MDP	Bone metastasis
$[^{99m}Tc]$Tc-mebrofenin	Hepatobiliary imaging
$[^{99m}Tc]$Tc-MIBI	Myocardial perfusion; glioblastoma
$[^{99m}Tc]$Tc-MPO	Myocardial perfusion
$[^{99m}Tc]$Tc-NOET	Myocardial perfusion
$[^{99m}Tc]$Tc-oxidronate	Altered osteogenesis; urothelial carcinoma
$[^{99m}Tc]$Tc-PnAO	Brain perfusion
$[^{99m}Tc]$Tc-Q12	Myocardial perfusion
$[^{99m}Tc]$Tc-tetrafosmin	Myocardial perfusion
$[^{64}Cu]$Cu-ATSM	Lung, cervical, and lung cancers
$[^{64}Cu]$Cu-PTSM	Myocardial perfusion
$[^{68}Ga]$Ga-Citrate	Wide variety of pathologies
$[^{68}Ga]$Ga-EDTMP	Bone metastasis
$[^{111}In]In\text{-}(oxinate)_3$	Platelet labeling
$[^{111}In]In\text{-}(tropolonate)_3$	Leucocyte labeling